

UC San Diego

UC San Diego Previously Published Works

Title

TPT sulfonate, a single, oral dose schistosomicidal prodrug: In vivo efficacy, disposition and metabolic profiling.

Permalink

<https://escholarship.org/uc/item/7b65k9qx>

Journal

International journal for parasitology. Drugs and drug resistance, 8(3)

ISSN

2211-3207

Authors

Wolfe, Alan R
Neitz, R Jeffrey
Burlingame, Mark
et al.

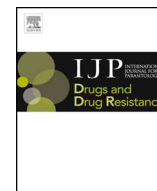
Publication Date

2018-12-01

DOI

10.1016/j.ijpddr.2018.10.004

Peer reviewed



TPT sulfonate, a single, oral dose schistosomicidal prodrug: *In vivo* efficacy, disposition and metabolic profiling

Alan R. Wolfe^{a,b}, R. Jeffrey Neitz^{b,c}, Mark Burlingame^c, Brian M. Suzuki^{b,d}, KC Lim^{b,d}, Mark Scheideler^e, David L. Nelson^f, Leslie Z. Benet^{a,b}, Conor R. Caffrey^{b,d,*}

^a Department of Bioengineering and Therapeutic Sciences, University of California San Francisco, 533 Parnassus Ave, San Francisco, CA, 94143, USA

^b Center for Discovery and Innovation in Parasitic Diseases, University of California, 1700 4th St, San Francisco, CA, 94158, USA

^c Department of Pharmaceutical Chemistry, University of California, 1700 4th St, San Francisco, CA, 94158, USA

^d Department of Pathology, University of California, 1700 4th St, San Francisco, CA, 94158, USA

^e Human First Therapeutics LLC, 9600 Dewitt Drive, Ste 1, Silver Spring, MD, 20910, USA

^f Pro-Rectoria of Research and Graduate Study, Federal University of the Valleys of Jequitinhonha and Mucuri, 39100-000, Diamantina, MG, Brazil

ARTICLE INFO

Keywords:

Schistosomiasis
Schistosoma
Anthelmintic
Alkylaminoalkanethiosulfuric acid
Drug metabolism
Drug disposition

ABSTRACT

Treatment of schistosomiasis relies precariously on just one drug, praziquantel (PZQ). In the search for alternatives, 15 S-[2-(alkylamino)alkane] thiosulfuric acids were obtained from a previous research program and profiled in mice for efficacy against both mature (> 42-day-old) and juvenile (21-day-old) *Schistosoma mansoni* using a screening dose of 100 mg/kg PO QDx4. One compound, S-[2-(*tert*-butylamino)-1-phenylethane] thiosulfuric acid (TPT sulfonate), was the most effective by decreasing female and male worm burdens by ≥ 90% and ≥ 46% (mature), and ≥ 89% and ≥ 79% (juvenile), respectively. In contrast, PZQ decreased mature female and male worm burdens by 95% and 94%, respectively, but was ineffective against juvenile stages. Against 7-day-old lung-stage worms, TPT sulfonate was only effective at twice the dose decreasing female and male burdens by 95 and 80%, respectively. Single oral doses at 400 and/or 600 mg/kg across various developmental time-points (1-, 7-, 15-, 21- and/or 42 day-old) were consistent with the QD x4 data; efficacy was strongest once the parasites had completed lung migration, and female and male burdens were decreased by at least 90% and 80%, respectively. *In vitro*, TPT sulfonate is inactive against the parasite suggesting a pro-drug mechanism of action. In mice, TPT sulfonate is fully absorbed and subject to rapid, non-CYP-mediated, first-pass metabolism that is initiated by desulfation and yields a series of metabolites. The initially-formed free thiol-containing metabolite, termed TP thiol, was chemically synthesized; it dose-dependently decreased *S. mansoni* and *Schistosoma haematobium* motility *in vitro*. Also, when administered as a single 50 mg/kg IP dose, TP thiol decreased 33-day-old *S. mansoni* female and male burdens by 35% and 44%, with less severe organomegaly. Overall, TPT sulfonate's efficacy profile is competitive with that of PZQ. Also, the characterization of a parasitocidal metabolite facilitates an understanding and improvement of the chemistry, and identification of the mechanism of action and/or target.

1. Introduction

Schistosomiasis is a flatworm disease endemic in areas where the infected snail vectors infest freshwater systems. With over 190 million people infected (Hotez, 2018) and as many as 700 million at risk (King, 2010), infections can last a lifetime and elicit progressive tissue and organ damage that results in pain and malaise. The disease detracts from school attendance and limits the capacity to perform manual labor, which remains critical in subsistence societies. Thus,

schistosomiasis is a direct contributor to poverty (Hotez et al., 2008; Utzinger et al., 2011).

Treatment and control of schistosomiasis relies on one drug, praziquantel (PZQ). Safe and reasonably effective against all the schistosome species infecting humans, PZQ is the lynchpin for the World Health Organization's (WHO) strategy of morbidity control via 'preventative chemotherapy.' Promulgation of this strategy has received a recent boost in interest by national and trans-national agencies that have reaffirmed a long-lasting and, indeed, expanding commitment to make

* Corresponding author. Center for Discovery and Innovation in Parasitic Diseases, Skaggs School of Pharmacy and Pharmaceutical Sciences, University of California San Diego, 9500 Gilman Ave, La Jolla, CA, 92093, USA.

E-mail address: ccaffrey@ucsd.edu (C.R. Caffrey).

<https://doi.org/10.1016/j.ijpddr.2018.10.004>

Received 26 July 2018; Received in revised form 19 October 2018; Accepted 22 October 2018

Available online 20 November 2018

2211-3207/ © 2018 The Authors. Published by Elsevier Ltd on behalf of Australian Society for Parasitology. This is an open access article under the CC BY-NC-ND license (<http://creativecommons.org/licenses/by-nc-nd/4.0/>).

out in accordance with a protocol (AN107779-01) approved by the Institutional Animal Care and Use Committee (IACUC) of the University of California San Francisco. UCSF-IACUC derives its authority for these activities from the United States Public Health Service (PHS) Policy on Humane Care and Use of Laboratory Animals and the Animal Welfare Act and Regulations (AWAR).

2.2. Synthesis of alkylaminoalkanethiosulfates

These compounds were prepared as previously described (Nelson et al., 1989; Moreira et al., 2000) by the opening of an epoxide with excess amine to form the amino alcohol. The amino group was protected by conversion to its hydrobromide salt, followed by the substitution of the hydroxyl group by bromine using phosphorus tribromide. Finally, the bromine atom was substituted through the reaction with sodium thiosulfate to furnish the final product. When the epoxide was not commercially available, it was prepared from the corresponding alkene via an epoxidation method described previously (Venturello et al., 1983). The evaluation of the purity and structure of the synthesized TPT sulfonate by HPLC, MS and MS/MS is described in the Supplementary Material.

2.3. *S. mansoni* life cycle

The acquisition, preparation and *in vitro* maintenance of *S. mansoni* schistosomula (somules or post-infective larvae) and adults have been described (Abdulla et al., 2009; Štefanić et al., 2010). We employed a Puerto Rican isolate of *S. mansoni* that is cycled between *Biomphalaria glabrata* snails and male Golden Syrian hamsters (Simonsen Laboratories; infected at 4–6 weeks of age) as intermediate and definitive hosts, respectively.

2.4. Phenotypic screening with *S. mansoni* somules and adults *in vitro*

Phenotypic screens involving *in vitro*-transformed somules were performed in 200 μ L Basch medium (Basch, 1981) in 96-well plates (Corning Inc., cat. # 3599), as described (Abdulla et al., 2009; Rojo-Arreola et al., 2014; Long et al., 2016). Phenotypic screens involving 42-day-old, mixed-sex parasites were performed in 24-well plates (Corning Inc., cat. # 3544) containing 2 ml Basch medium and 4% FBS using five worm pairs per well (Abdulla et al., 2009; Long et al., 2016, 2017). Compounds were added in a volume of up to 1 μ L DMSO. Incubations were maintained for 3 day at 37 °C under 5% CO₂. Parasite responses to chemical insult were observed at various time-points using a Zeiss Axiovert 40 C inverted microscope and recorded using a constrained nomenclature of phenotype ‘descriptors’ (e.g., rounding, degeneration, overactivity and changes in motility) as described (Abdulla et al., 2009; Glaser et al., 2015; Long et al., 2016, 2017). WormAssay (Marcellino et al., 2012), as modified to measure adult schistosome motility (Long et al., 2017; Weeks et al., 2018), was also employed.

2.5. Murine model of *S. mansoni* infection

Infections with *S. mansoni* were initiated by the subcutaneous injection of 150 cercariae in water into 3–5-week-old female Swiss Webster mice. At various times post-infection, compound was administered orally (PO) by gavage once daily for up to four successive days (QDx4) using 2.5% Kolliphor (Cremophor) EL as the vehicle (n = 3–6 mice). We considered this treatment regimen as sufficient to record any compound efficacy given that the desired target product profile for new-anti-schistosomal drugs calls for short course, preferably, single-dose, therapy (Nwaka and Hudson, 2006; Caffrey, 2007). At various time points post-treatment (see experimental details and results outlined in Table S1), mice were euthanized with an intraperitoneal injection of 50 mg/kg sodium pentobarbital and adult worms were harvested by reverse perfusion of the hepatic portal system

(Pellegrino and Siqueira, 1956; Duvall and DeWitt, 1967; Colley and Wikel, 1974; Abdulla et al., 2007) in RPMI 1640 medium containing 50U/1 heparin.

Compound efficacy was measured using the primary criterion of reduction in worm (male and female) burden. The current anti-schistosomal drug, PZQ, was used as a drug control, as described (Abdulla et al., 2007, 2009). Also, any amelioration of pathology, as evidenced by decreased liver and spleen weights vs. vehicle controls (Abdulla et al., 2007), was recorded in Table S1. This Excel workbook also contains observation notes on worm size and condition upon recovery.

2.6. Cytotoxicity counter screens

Bovine embryo skeletal muscle (BESM; (Engel et al., 1985), mouse myoblast (C2C12 (Blau et al., 1985); and human hepatoma HuH-7 cells (Nakabayashi et al., 1984) were cultured in RPMI 1640 medium supplemented with 10% heat-inactivated fetal calf serum (FCS) and 1% penicillin/streptomycin at 37 °C in 5% CO₂. Cells were seeded into 24-well plates and grown to 50–60% confluence. Freshly prepared compound in DMSO was added to the cells to yield final concentrations of 5, 10, 20 and 40 μ M. Assays were set up in triplicate with DMSO controls. After 24 h, cells were fixed o/n with an equal volume of PBS containing 10% paraformaldehyde. Cells were then washed in PBS containing 0.1% sodium azide and 1 μ g/ml 4',6-diamidino-2-phenylindole (DAPI). Nuclei were counted across 5–10 fields of view/well using a Zeiss Axiovert 40 C inverted microscope fitted with a 20x objective lens and the Zeiss filter set 02 (365/420 nm). Total nuclei counts per concentration were expressed as a percentage relative to DMSO controls.

2.7. Positive ion-mode electrospray tandem MS of TPT sulfonate and its metabolites in mouse plasma and mouse hepatocyte digests

The principal fragments of m/z 290 TPT sulfonate observed using an API 4000 LC-MS/MS system (SCIEX, Framingham, MA) (see description under Results) are m/z 234, 135, 120 and 91. Thus, searches for metabolites could be carried out with, for example, m/z 56 neutral loss scanning (NLS) or m/z 91 precursor ion scanning (PIS). Metabolite discovery was carried out primarily using m/z 56 NLS, from m/z 100 to 650. Multiple reaction monitoring for quantitation of TPT sulfonate and its m/z 256 and 176 metabolites used the parent \rightarrow daughter ion transitions m/z 290.1 \rightarrow 234.1, 256.1 \rightarrow 200.1 and 176.1 \rightarrow 120.1, respectively. MS settings were declustering potential (DP), 60 V; collision energy (CE), 19 eV; collision cell exit potential (CXP), 31 V; entrance potential (EP), 10 V; collision gas (collisionally activated dissociation, CAD), 12 psi; curtain gas (CUR), 16 psi; gas 1 (ion source nebulizer gas, GS1), 30 psi; gas 2 (ion source heater gas, GS2), 40 psi; ion spray voltage (IS), 5500 V and temperature (TEM), 500 °C.

The column employed was a 25 \times 0.46 cm Beckman Ultrasphere 5 μ m 100 Å C8. The mobile phases were A = 60% and B = 100% methanol/water, containing 0.1% acetonitrile, 0.1% formic acid and 0.16 g/L NH₄OAc. The gradient was 0–2 min, 0% B; 2–6 min, linear ramp to 80% B; 6–7 min, 80% B; 7–8 min, linear ramp to 0% B; 8–12 min, 0% B; all at a flow rate of 0.6 ml/min. Retention times were 5.6, 5.8, 6.2 and 6.4 min for TPT sulfonate and the metabolites at m/z 256, m/z 176 and m/z 210, respectively.

2.8. High mass accuracy MS of TPT sulfonate and the dimer of the thiol metabolite

To aid in molecular characterization, high mass accuracy mass spectra (sufficiently accurate to establish atomic composition) were obtained for samples of TPT sulfonate, the m/z 417 dimer of the synthetic m/z 210 thiol and their daughter ions in positive ion MS/MS mode. Decomposition products of the m/z 417 dimer were also evaluated in MS mode. These spectra were obtained from a linear ion trap-Orbitrap instrument (LTQ Orbitrap, Thermo Fisher Scientific) with the

samples being introduced by infusion.

2.9. Stability of TPT sulfonate in mouse plasma

For comparison with pharmacokinetic results, the stability of 400 μ M TPT sulfonate in mouse plasma containing 1% DMSO was measured at 37 °C using plasma from female Balb/C mice (Biological Specialty Corp., Colmar PA). Small aliquots of the sample were injected directly into an Agilent 1100 HPLC using UV detection.

2.10. Digestion of TPT sulfonate by mouse microsomes

The susceptibility of TPT sulfonate to digestion by liver microsomal cytochrome P450 (CYP) and UDP-glucuronosyltransferase (UGT) enzymes was evaluated at 37 °C using female CD1 mouse liver (pool of 400) microsomes (Xenotech, Lenexa, KS) in 50 mM potassium phosphate, pH 7.4, and 4 μ M TPT sulfonate (adding 0.1% DMSO).

For CYP digestion tests, the above assay solution also contained 1.0 mM NADPH as a cofactor (except in the control). All components except the NADPH were pre-incubated for 5 min before initiating the reaction. The cysteine protease inhibitor, K11777 (N-Methyl-Pip-F-hF-VS Φ ; (Jacobsen et al., 2000), served as a positive control.

For glucuronidation tests, the above assay solution also contained 1 mM MgCl₂, 0.15 mg/ml Brij 58 (a micelle-forming detergent), 5 mM saccharolactone (β -glucuronidase inhibitor) and 5 mM uridine diphosphate glucuronic acid trisodium salt (UDPGA). All components except the substrate and UDPGA were pre-incubated for 15 min. Substrate was then added and after 5 min the reaction was initiated. 1-Naphthol served as a positive control.

In both assays, 100 μ L aliquots of the reaction mixture were removed at various time points, mixed with 100 μ L of cold methanol and placed on dry ice. Samples were then centrifuged for 5 min at 12,000 \times g and the supernatants were analyzed with an Agilent 1100 HPLC as described above.

2.11. Digestion of TPT sulfonate by rodent hepatocytes and anti-schistosomal activity

Rodent hepatocytes were used to further assess the metabolic stability of TPT sulfonate. Hepatocytes were isolated from a 5-week-old female Swiss Webster mouse or a 12-week old female Sprague-Dawley rat and purified by Percoll gradient (Kraemer et al., 1986). Mouse and rat hepatocytes (3.0×10^6 cells/ml in the experiments used for efficacy testing) were incubated in Williams' medium E, pH 7.4, containing 4 mM glutamine and 750 μ M TPT sulfonate (DMSO final concentration was 0.16%). Controls comprised (i) hepatocytes incubated without TPT sulfonate and (ii) 750 μ M TPT sulfonate added to Williams' medium E but without hepatocytes. Incubations were maintained at 37 °C with shaking and bubbling of 5% CO₂:O₂. After 30 min, the medium was withdrawn, centrifuged for 1 min at 12,000 \times g and frozen at –80 °C until use. The expected extent of TPT sulfonate digestion in 30 min (based on the data in Figure S1E) is ~100% and ~75% for the mouse and rat hepatocytes, respectively.

Before incubating with adult schistosomes, rat hepatocyte medium was filtered through a 0.2 μ M syringe filter (Millipore). Medium (100, 200, 400 or 700 μ L) was added to 200 μ L complete Basch medium containing five adult *S. mansoni* pairs, or, in one experiment, four adult *S. haematobium* males (supplied by Dr. Michael H. Hsieh, then at the Dept. of Pathology, Stanford University, Palo Alto, CA). Phenotypic changes in the worms and/or changes in worm motility were assessed at 2 and 18 h as described above.

2.12. Initial pharmacokinetics (PK) study in mice

The metabolic stability of TPT sulfonate and the identities and stabilities of the metabolites formed were investigated in 5 week-old,

female Swiss Webster mice. TPT sulfonate was formulated in 2.5% Kolliphor EL and administered orally (PO) by gavage (150 μ L) at 100 mg/kg. Blood samples were collected in tubes containing K₂EDTA via retro-orbital bleeding at 0.5, 2.0 and 4.0 h after dosing (n = 3 per time point).

2.13. Extended PK study in mice

To more fully characterize the formation and stability of TPT sulfonate and its m/z 256, 210 and 176 metabolites, a larger PK study was conducted using the contract research organization (CRO), WuXi AppTec Co. Ltd. (Shanghai). Female Swiss Webster (CFW) mice (~20 g; Charles River) that had been fasted overnight were dosed intravenously (IV) via the tail vein (4 mice, 15 mg/kg) or PO (8 mice, 100 mg/kg). TPT sulfonate was formulated as a solution in 10% DMSO, 60% PEG-400, 30% water (IV) or as a suspension in 2% Tween 80 in 0.5% hydroxypropyl methylcellulose (PO). For the IV route of administration, 25 μ L blood samples were withdrawn after 5, 15, and 30 min, and 1, 2, 4, 8 and 24 h. For the PO route, samples were similarly withdrawn but omitting the 5 min time point. Blood was collected from the sub-mandibular or saphenous vein, or via cardiac puncture, and treated with K₂EDTA anticoagulant. Samples were then cooled to 4 °C and centrifuged for 10 min at 4500 \times g. The resulting blood plasma was frozen on dry ice and stored at –80 °C.

Thawed samples were prepared for analysis by combining 8 μ L of plasma with 80 μ L of 1:1 methanol:acetonitrile containing 0.1% formic acid and 200 ng/ml tolbutamide. The mixture was vortexed for 1 min and centrifuged at room temperature for 15 min at 15,900 \times g. An aliquot (80 μ L) of the supernatant was combined with 160 μ L of water containing 0.1% formic acid, vortexed for 10 min and then centrifuged for 10 min at 3200 \times g and 4 °C. TPT sulfonate and its m/z 176, 210 and 256 metabolites were then analyzed by LC/MS/MS via their m/z 56 neutral-loss-daughter ions using an ACQUITY UPLC[®] (Waters, Milford MA) with a 1.7 μ m, 2.1 \times 50 mm Waters BEH C18 column and an API 4000 mass spectrometer in positive ion electrospray mode. The mobile phase was a combination of mixture A, consisting of 0.1% formic acid in 19:1 water:acetonitrile, and mixture B, comprising 0.1% formic acid in 1:19 water:acetonitrile. The 1.8-min gradient went from 1% B to 45% B, with a curve setting of 6, at a flow rate of 0.6 ml/min. Retention times were 1.15, 0.82, 0.79 and 1.10 min for TPT sulfonate, m/z 256 metabolite, m/z 176 metabolite and m/z 210 metabolite, respectively.

The internal standard used was tolbutamide, using the 271.1 \rightarrow 155.0 transition. MS settings were CXP, 12 V; EP, 10 V; CAD, 10 psi; CUR, 20 psi; GS1, 50 psi; GS2, 50 psi; IS, 5500 V; TEM, 500 C. DP and CE were, respectively, 74 V and 19 eV for m/z 56 neutral loss transitions, and 63 V and 26 eV for the 271.1 \rightarrow 155.0 tolbutamide transition.

2.14. Software packages

PK data were analyzed using Phoenix WinNonlin 6.2.1 (Certara, Princeton NJ). Predictions of sites and relative extents of cytochrome P-450 oxidative metabolism were made with MetaSite 4.0.4 (Molecular Discovery, Borehamwood, United Kingdom) (Cruciani et al., 2013). Additional molecular physicochemical and ADME parameter predictions were made with VolSurf+ 1.0.7.1 (Molecular Discovery) (Cruciani et al., 2000a, 2000b).

3. Results

3.1. Thiosulfates are inactive against *S. mansoni* in vitro

The 15 aryl- and alkylthiosulfates (structures shown in Table 1) received from Dr. Nelson were tested for *in vitro* activity against somules and adult *S. mansoni* using established protocols (Abdulla et al., 2009; Rojo-Arreola et al., 2014; Long et al., 2016, 2017; Weeks et al., 2018). None of the compounds induced obvious phenotypic changes at

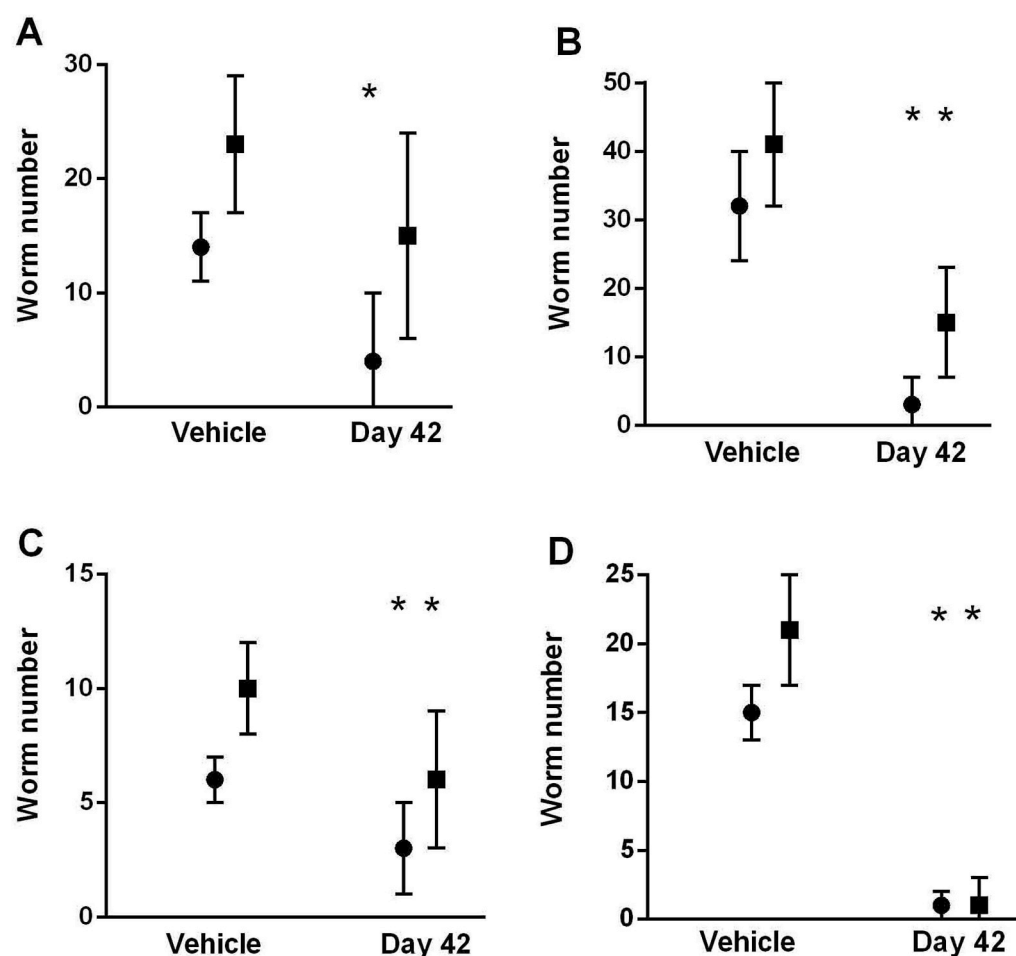


Fig. 1. Efficacy of those most potent compounds of the 15 thiosulfates tested against mature *S. mansoni* infections in mice. Compounds 1, 2 and 8 and PZQ (A–D respectively) were administered orally by gavage at 100 mg/kg QDx4 in 150 μ L 2.5% Kolliphor EL 42 days post-infection (dpi) with 150 *S. mansoni* cercariae. Means \pm SD of female (circle) and male worms (squares) recovered by perfusion from mice ($n = 3$ –6 per group) at 62 (A), 56 (B), (C) 59 and 60 dpi (D), respectively, are indicated. Significance relative to vehicle controls for each sex was measured using the Student's unpaired *t*-test with a two-tailed distribution; significance ($p < 0.05$) is indicated by asterisks. See Table S1 (worksheets 4, 8, 5 and 14, respectively) for further details on data per mouse.

concentrations of up to 10 μ M over 3 days.

3.2. Screening of thiosulfates against mature *S. mansoni* infections in mice identifies one compound (TPT sulfonate) with efficacy similar to that of PZQ

Compound efficacy, i.e., reductions in female and male worm burdens, in a mouse model of *S. mansoni* infection employed a screening dose of 100 mg/kg PO QDx4 to target mature 42-day-old parasites. The data for the 15 compounds are summarized in Table 1. The complete set of data, as indicated in the appropriate figure legends, regarding changes in worm burdens, and weights of the liver and spleen (as a metrics for disease-associated pathology (Abdulla et al., 2007) and references therein) is presented in Table S1.

Of the 15 compounds, compounds 1 [(2-isopropylamino)-1-phenyl-1-ethanethiosulfuric acid], 2 [(2-*tert*-butylamino)-1-phenyl-1-ethanethiosulfuric acid or TPT sulfonate] and 8 [(2-isopropylamino)-1-octanethiosulfuric acid] were the most effective in reducing worm burdens at 42 days post-infection (dpi) (Table 1; Fig. 1) and of these TPT sulfonate was the best. Thus, Compound 1 decreased female and male worm burdens by at least 60% and 37%, respectively, in two separate experiments, (one shown in Fig. 1A). Compound 2 reduced female and male worm burdens by at least 90% and 46%, respectively, in two separate experiments (one experiment shown in Fig. 1B). Also, worms recovered by perfusion after exposure to 2 (TPT sulfonate) were noticeably shorter and less massive (Fig. 2). Finally, compound 8 decreased female and male worm burdens by 50% and 40%, respectively (Fig. 1C). For comparison, the same QDx4 dosing at 42 dpi with the current anti-schistosomal drug, PZQ, decreased female and male worm burdens by 95% and 94%, respectively (Table 1; Fig. 1D).

3.3. Compound 2 (TPT sulfonate) kills 21 day-old juvenile parasites that are least sensitive to PZQ

Having established the superior efficacy of TPT sulfonate among the 15 compounds tested at 42 dpi, we next assessed the compounds' efficacy using the same 100 mg/kg QDx4 dosing regimen at 21 dpi – a time point in the parasite's development at which PZQ is least effective (Keiser et al., 2009 #1030; Sabah et al. (1986) #38; Gönner and Andrews., 1977 #548). The data are summarized in Table 1 and the complete set of data is presented in Table S1. TPT sulfonate was again the most effective compound whereby female and male worm burdens were decreased by at least 89% and 79%, respectively, in two separate experiments (one shown in Fig. 3A). The 2-sec-butyl analog (14) of TPT sulfonate was the next most effective, decreasing female and male worm burdens by 72% and 61%, respectively (Table 1; Table S1 worksheet 6). Compound 1 was moderately effective, decreasing female and male worm burdens by 62% and 60%, respectively (Table 1; Table S1 worksheet 9). By comparison, PZQ at 100 mg/kg QDx4 was essentially inactive against 21-day-old parasites (Fig. 3C).

Focusing now on TPT sulfonate, we tested its efficacy at 100 mg/kg QDx4 against 7- and 11-day-old *S. mansoni* in mice, i.e., when the parasite is in the midst of and has completed its migration through the lungs, respectively ((Rheinberg et al., 1998) and references therein). TPT sulfonate was much less effective against 7-day-old lung-stage parasites, decreasing female burdens by 40% and those of males by 12% (Table 1; Fig. 3A). In contrast, 11-day-old parasites were markedly susceptible to TPT sulfonate whereby female and male worm numbers were decreased by 83% and 81%, respectively (Table 1; Fig. 3B). For comparison, PZQ at 7 dpi, decreased female and male worm burdens by 58% and 44% (Table 1; Fig. 3C).

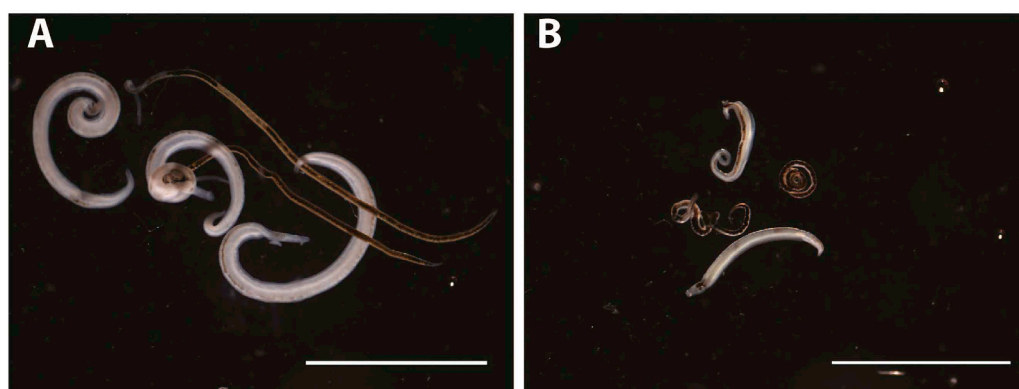


Fig. 2. Effect of TPT sulfonate (compound 2) on worm length and mass. TPT sulfonate was administered orally by gavage to mice at 100 mg/kg QDx4 in 150 μ L 2.5% Kolliphor EL 42 days post-infection (dpi) with 150 *S. mansoni* cercariae. Vehicle control worms (A) and those exposed to TPT sulfonate (B) were recovered by perfusion at 56 dpi. Worms exposed to TPT sulfonate are approximately 50% shorter and less massive. Males can be distinguished from females by being thicker and paler in color. Bars = 0.6 cm.

For the series of 15 thiosulfates as a whole, a rudimentary SAR could be demonstrated. Efficacy was greatest among compounds with a phenyl R1 group placed proximal to the sulfur terminus (compounds 1, 2, 7 and 14) with *tert*-butyl > isopropyl > *sec*-butyl > cyclohexyl being preferred alpha to the amino terminus (R3). Compounds 8–11, which lack the phenyl R1 group and have noncyclic aliphatic $n \geq 4$ R2 and propyl R3 substituents, show a trend for statistically significant reductions in worm burdens, principally at the 21-day time point. The similar compound series, 3–6, with bulkier butyl R3 substituents, showed at best weak and statistically insignificant activity. A cyclohexyl R3 substituent seems to abolish activity.

The 3-dimensional configurations and molecular properties of the thiosulfate series were predicted by VolSurf+ (Cruciani et al., 2000b). The software indicated the presence of internal hydrogen bonds between the thiosulfate and the amine. This was true for both the charged (pH 7.0) and uncharged forms of the molecules. Evaluation of the properties of the uncharged molecules (which are generally the membrane-crossing species) showed that the presence of internal H-bonds

significantly increased predicted measures of skin permeability, Caco-2 monolayer permeability and blood-brain barrier permeability (Cruciani et al., 2000a); p values were < 0.0001, < 0.0001 and 0.0002, respectively. For example, the mean predicted increase in log brain/blood distribution was 0.075 ± 0.048 (about a 20% increase in the ratio). No significant correlation with antiparasitic activity (using the average values for different time points) was found for estimates of properties such as log P, solubility, permeability, susceptibility to CYP3A4 metabolism or protein binding. Among the molecular descriptors calculated by VolSurf+, the strongest correlations with efficacy were found for four that are related to the solubility versus pH profiles (L1LgS – L4LgS). They represent how closely these profiles correlate with Legendre polynomials of grades 1–4 (useful in distinguishing compounds similar in solubility but with different pH-dependent profiles, or vice versa). In these cases, the R value of the correlation was in the 0.71–0.73 range, and the correlation was present in both the phenyl-bearing and non-phenyl-bearing members of the series. However, given the large number (128) of molecular properties evaluated, and the

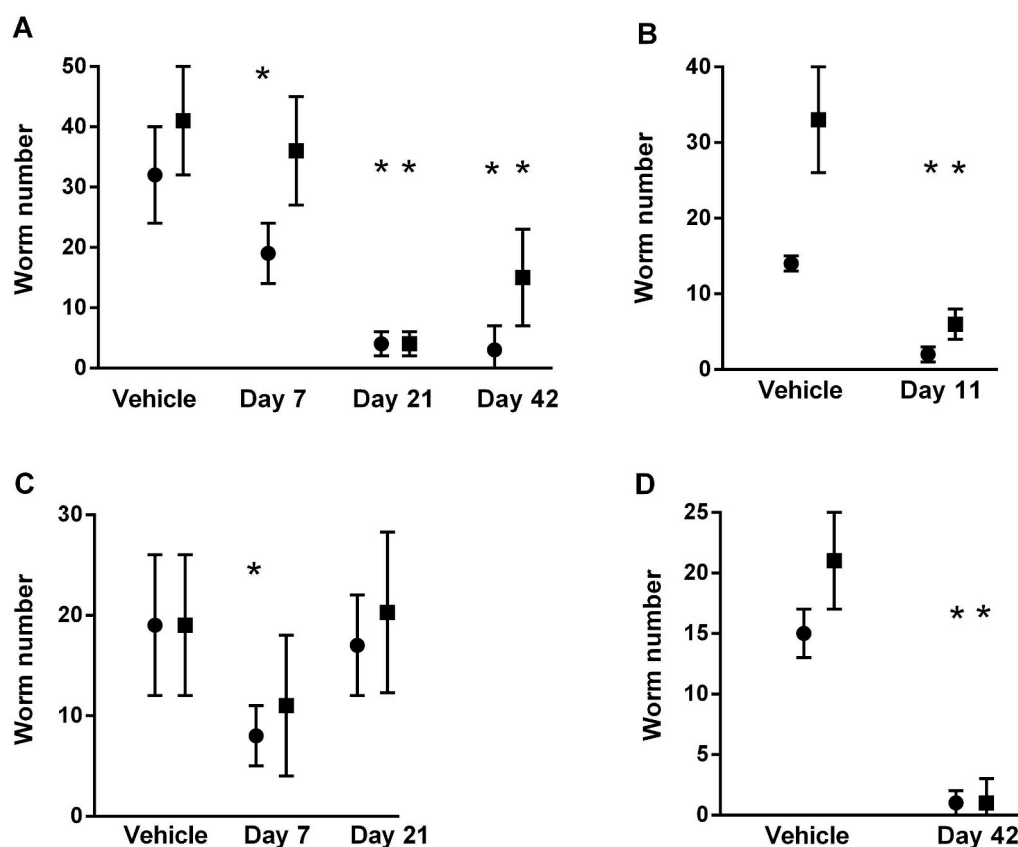


Fig. 3. Effect of worm age on efficacy of TPT sulfonate as compared to PZQ in mice infected with *S. mansoni*. TPT sulfonate (compound 2) was administered orally by gavage at 100 mg/kg QDx4 in 150 μ L 2.5% Kolliphor EL at 7, 21 and 42 (A), and 11 days post-infection (dpi) (B) with 150 *S. mansoni* cercariae. PZQ was administered under the same conditions at 7 and 21 (C), and 42 dpi (D) with 150 *S. mansoni* cercariae. Means \pm SD of female (circle) and male worms (squares) recovered from mice ($n = 3$ –6 per group) 56 (A), 35 (B), 49 (C) and 60 dpi (D) are indicated. Significance relative to vehicle controls for each sex was measured using the Student's unpaired t -test with a two-tailed distribution; significance ($p < 0.05$) is indicated by asterisks. The data shown for vehicle and 42 dpi in panels A and D are the same as those shown in Fig. 1B and D, respectively, and are provided here for easier comparisons. See also Table S1 (worksheets 2, 8 and 9 for TPT sulfonate, and worksheets 14 and 15 for PZQ) for details.

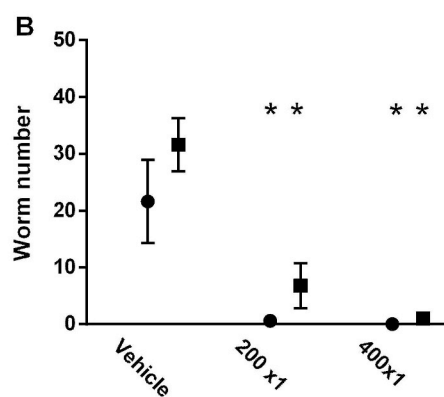
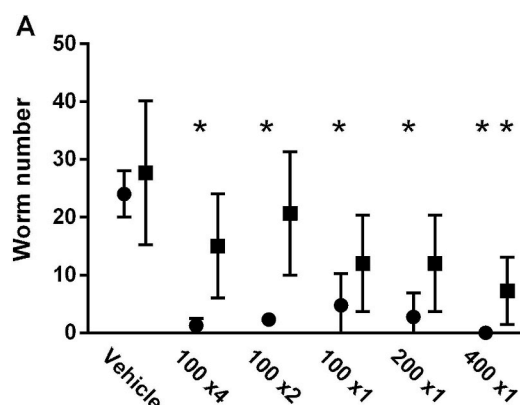


Fig. 4. Dose-ranging of TPT sulfonate indicates that mature female *S. mansoni* are more susceptible than males. (A) TPT sulfonate was administered orally by gavage at the doses (mg/kg) indicated in 150 μ L 2.5% Kolliphor EL at 42 days post-infection (dpi) with 150 *S. mansoni* cercariae. Means \pm SD of female (circle) and male worms (squares) recovered from mice ($n = 3$ –6 per group) 56 dpi are indicated. (B) For comparison, PZQ was administered at the doses indicated under the same conditions. Significance relative to vehicle controls for each sex was measured using the Student's unpaired *t*-test with a two-tailed distribution; significance

($p < 0.05$) is indicated by asterisks. See Table S1 (worksheets 10 and 17 for TPT sulfonate and PZQ, respectively) for details.

limited structural diversity in the molecule set, the significance and generality of these correlations is not clear. In contrast, a weaker correlation seen between efficacy and volume of distribution ($R = 0.61$) was phenyl-dependent (absent in both the phenyl-bearing and non-phenyl-bearing molecule sets).

3.4. TPT sulfonate is an effective schistosomicide at single oral doses

Having defined the oral efficacy of TPT sulfonate against key developmental stages of *S. mansoni* in mice using the initial screening dose of 100 mg/kg QDx4, we next tested a number of single (100, 200 and 400 mg/kg) and multiple dosing regimens (100 mg/kg QDx2 and 100 mg/kg QDx4) against mature 42-day-old infections to determine the regimen that produces the greatest reductions in worm burdens. As indicated in Fig. 4 and consistent with the foregoing data, females were more susceptible to TPT sulfonate irrespective of dosing regimen. Thus, the reductions ranged from 83% at the single 100 mg/kg dose to 100% at the single 400 mg/kg dose, whereas for males, a maximum reduction of 74% at the single 400 mg/kg dose was measured (Fig. 4A). By comparison, PZQ decreased female and male worm burdens by 97% and 78%, and 100 and 97%, respectively at single oral doses of 200 and 400 mg/kg (Fig. 4B). Overall, at the highest single dose of 400 mg/kg, TPT sulfonate is as effective as PZQ in removing female worms, whereas male worms are somewhat less susceptible to TPT sulfonate.

In an attempt to improve the single dose efficacy of TPT sulfonate, we compared dosing at 400 and 600 mg/kg over a range of time points (1, 7, 15, 21 and 42 dpi) that spans the entire development of the parasite (Fig. 5). As noted earlier for the 100 mg/kg QDx4 dosing

regimen, the 400 and 600 mg/kg single doses of TPT sulfonate were not significantly effective against 7-day-old lung-stage parasites ($\leq 38\%$ and $\leq 32\%$ reductions in female and male burdens, respectively; Fig. 5A). In contrast, 21 day-old parasites were highly susceptible with no distinguishable differences between the 400 and 600 mg/kg doses, i.e., 95 and 91%, and 97 and 95% reductions in female and male burdens, respectively. Likewise, for mature 42 day-old worms, TPT sulfonate was equally effective at the 400 and 600 mg/kg doses, decreasing female and male burdens by 100 and 85%, and by 100 and 81%, respectively.

As shown in Fig. 5B for the 600 mg/kg dose, one-day-old larvae (presumably located in the skin (Rheinberg et al., 1998)) were not susceptible to TPT sulfonate; also, lung-stage parasite burdens at 7 dpi were non-significantly decreased by 28% (both sexes). In contrast, 15-day-old, post-lung-migratory worms were highly sensitive as reductions of 89% and 92% for females and males, respectively, were measured.

3.5. Increasing the QDx4 regimen from 100 mg/kg to 200 mg/kg improves killing of lung-stage worms

In a final effort to improve efficacy against 7-day-old, lung-stage *S. mansoni*, and noting that the original 100 mg/kg QDx4 regimen had some significant impact on female, but not male worm burdens (Fig. 3; reductions of 40% and 12%, respectively), we doubled the daily dose of TPT sulfonate to 200 mg/kg QDx4. This regimen markedly improved efficacy by decreasing female and male worm burdens by 95 and 80%, respectively (Fig. 6). Thus, lung-stage worms are susceptible to TPT sulfonate at the higher dose.

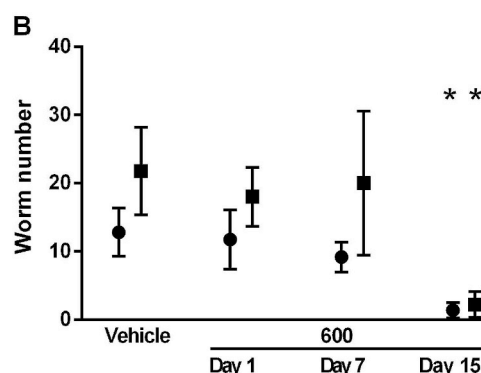
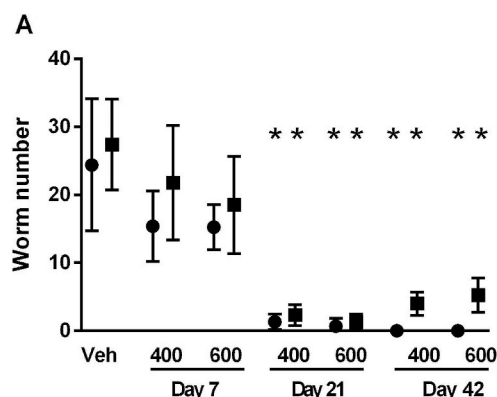


Fig. 5. Increasing the single oral dose of TPT sulfonate can cure mice infected with *S. mansoni*: again efficacy depends on worm age. TPT sulfonate was administered orally by gavage at the doses (mg/kg) indicated in 150 μ L 2.5% Kolliphor EL at 7, 21 and 42 days post-infection (dpi) (A), and 1, 7 and 15 dpi (B) with 150 *S. mansoni* cercariae. Means \pm SD of female (circle) and male worms (squares) recovered from mice ($n = 3$ –6 per group) 52 (A) and 44 dpi (B) are indicated. Significance relative to vehicle controls for each sex was measured using the Student's unpaired *t*-test with a two-tailed distribution; significance ($p < 0.05$) is indicated by asterisks. See Table S1 (worksheets 11 and 12 for (A) and (B), respectively) for details.

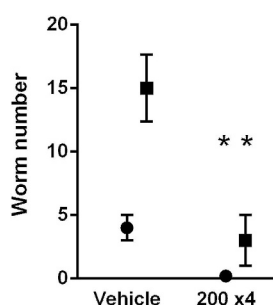


Fig. 6. Increasing the dose of TPT sulfonate from 100 QDx4 to 200 QDx4 significantly improves efficacy against 7 day-old lung worms. TPT sulfonate was administered orally by gavage at the dose 200 mg/kg QDx4 in 150 μ L 2.5% Kolliphor EL at 7 days post-infection (dpi) with 150 *S. mansoni* cercariae. Means \pm SD of female (circle) and male worms (squares) recovered from mice ($n = 3$ –5 per group) 57 dpi are indicated. Significance relative to vehicle controls for each sex was measured using the Student's unpaired *t*-test with a two-tailed distribution; significance ($p < 0.05$) is indicated by asterisks. See Table S1 (worksheet 13) for details. Also, compare these data to those shown for 100 mg/kg QDx4 in Fig. 1A.

3.6. Summary of TPT sulfonate's in vivo efficacy

In its single, oral dose efficacy, the data so far suggest that: (i) TPT sulfonate is comparable to PZQ in removing mature 42 day-old female worms, but it is somewhat less effective against mature males (e.g., 74–85% worm reductions vs. 97% for PZQ at 400 mg/kg); (ii) TPT sulfonate is particularly effective against juvenile 21 day-old parasites ($\geq 91\%$ worm kill), i.e., those parasites that are least responsive to PZQ; (iii) skin- (1 dpi) and lung-stage worms (7 dpi) are the least susceptible to TPT sulfonate, and for the later time point, the efficacy measured is less than that of PZQ and (iv) TPT sulfonate's efficacy markedly improves from 7 to 11 (or 15) dpi, coincident with the completion of migration of *S. mansoni* from the lungs and its establishment in the mesenteric venous system (Rheinberg et al., 1998). Finally, although lung-stage parasites are less susceptible to TPT sulfonate than older parasites, they are not refractory because increasing the QDx4 dosing regimen from 100 to 200 mg/kg markedly improves worm killing. The data generated here for PZQ at 7, 21 and 42 dpi are consistent with those previously reported (Gönnert and Andrews, 1977; Sabah et al., 1986; Keiser et al., 2009). Regardless of the dosing regimen employed with TP sulfonate, mice did not exhibit signs of stress, e.g., hunched posture, agitation, lack of feeding or drinking.

3.7. TPT sulfonate is stable in plasma and to digestion by microsomes, but is rapidly metabolized by hepatocytes

TPT sulfonate is relatively stable in mouse plasma, degrading by just over 50% after 40 h at 37 °C (Figure S1A). It is also resistant to

biotransformation by mouse liver microsomes: clearance in the presence and absence of NADPH was 0.19 and 0.15 ml/h/mg, respectively, i.e., digestion was very slow and mostly non-CYP mediated (Table 2; Figure S1B). No significant TPT sulfonate transformation was measured in the glucuronidation assay (Table 2; Figure S1C).

In contrast to the microsomal assays, TPT sulfonate was readily metabolized by intact hepatocytes from either mouse or rat (Table 2; Figures S1D, S1E). The clearance of TPT sulfonate by mouse hepatocytes was 1.9 ml/h/million cells (32 μ L/min/million cells; Figure S1D). This value is high relative to those for other compounds in the literature (Lau et al., 2002). The hepatocyte contents of mouse and rat livers are known to be similar (Sohlenius-Sternbeck, 2006). If we assume the microsome content of mouse hepatocytes is also similar to the rat value (0.37 mg/million cells, based on 61 mg/g and 163×10^6 cells/g (Smith et al., 2008), the mouse hepatocyte clearance result is equivalent to 5.1 ml/h/mg microsomes, over 20 times the total microsomal clearance and over 100 times the CYP-mediated or UDP-glucuronosyltransferase-mediated microsomal clearance (Table 2). Thus, the metabolism of TPT sulfonate by mouse hepatocytes appears not to be mediated by enzymes of these classes.

3.8. Transformation of TPT sulfonate by hepatocytes is required for expression of anti-schistosomal activity, incl. against *S. haematobium*

Primary rat hepatocyte cultures in Williams' medium E were incubated for 30 min in the presence or absence of 750 μ M TPT sulfonate. Negative controls comprised either TPT sulfonate incubated in Williams' medium E but omitting the hepatocytes or hepatocytes incubated in the absence of TPT sulfonate. Medium (100, 200, 400 or 700 μ L) was then withdrawn and added to adult *S. mansoni* in 200 μ L Basch medium. Worms were observed microscopically and motility measured using WormAssay after 2 and 18 h.

No effects on worms were recorded in the presence of 100 or 200 μ L Williams' medium E conditioned by hepatocytes in the presence of TPT sulfonate. However, worms incubated with 400 and 700 μ L of the same medium were clearly stressed (Fig. 7). Thus, after 2 h, worm motility was decreased by approximately 90–95% (Fig. 7A), and males and females had become uncoupled with an inability to adhere to the floor of the well. After 18 h, worm motility remained severely depressed and, observationally, worms were barely moving with tegumental (surface) damage being also apparent (Fig. 7B, C), a finding that conceivably would lead to immune-mediated clearance of the worms *in vivo* as postulated for PZQ (Andrews, 1985; Brindley and Sher, 1987; Doenhoff et al., 1987). In a single experiment, the depressed motility and other phenotypic effects observed microscopically for *S. mansoni* after 2 and 18 h of incubation in the presence of 400 and 700 μ L hepatocyte-conditioned medium were also noted for adult *S. haematobium* males. For all experiments, both of the negative control conditions (700 μ L medium) did not alter worm motility or appearance (Fig. 7D, E).

Table 2

Relative rates of TPT sulfonate digestion by mouse microsomes and hepatocytes.

Assay type	k , (h^{-1})	Microsomes (mg/ml)	<i>In vitro</i> clearance (ml/h/mg)
Mouse microsomal glucuronidation ^a	0.07	3.5	0.02
Mouse microsomal CYPs ^b	0.1	3.33	0.04
Mouse microsomes, non-specific ^c	0.5	3.33	0.15
Mouse hepatocytes	4.6	0.90 ^d	5.1

In vitro clearance values of TPT sulfonate expressed relative to mouse liver microsome concentration (or microsome content, for hepatocytes). Values of the exponential decay constant k were obtained by fitting the data to the equation: TPT sulfonate concentration = $a \cdot \exp(-k \cdot t)$. *In vitro* clearance is then given as k /microsome concentration (the calculation assumes enzyme saturation is negligible). See Figures S1B–S1D for digestion plots.

^a Value with UDPGA and other glucuronidation assay components (see Materials and Methods).

^b Value with NADPH minus value without.

^c Without cofactor NADPH or other additions.

^d Based on the microsome equivalent of rat hepatocytes, 0.37 mg/million cells (Smith et al., 2008).

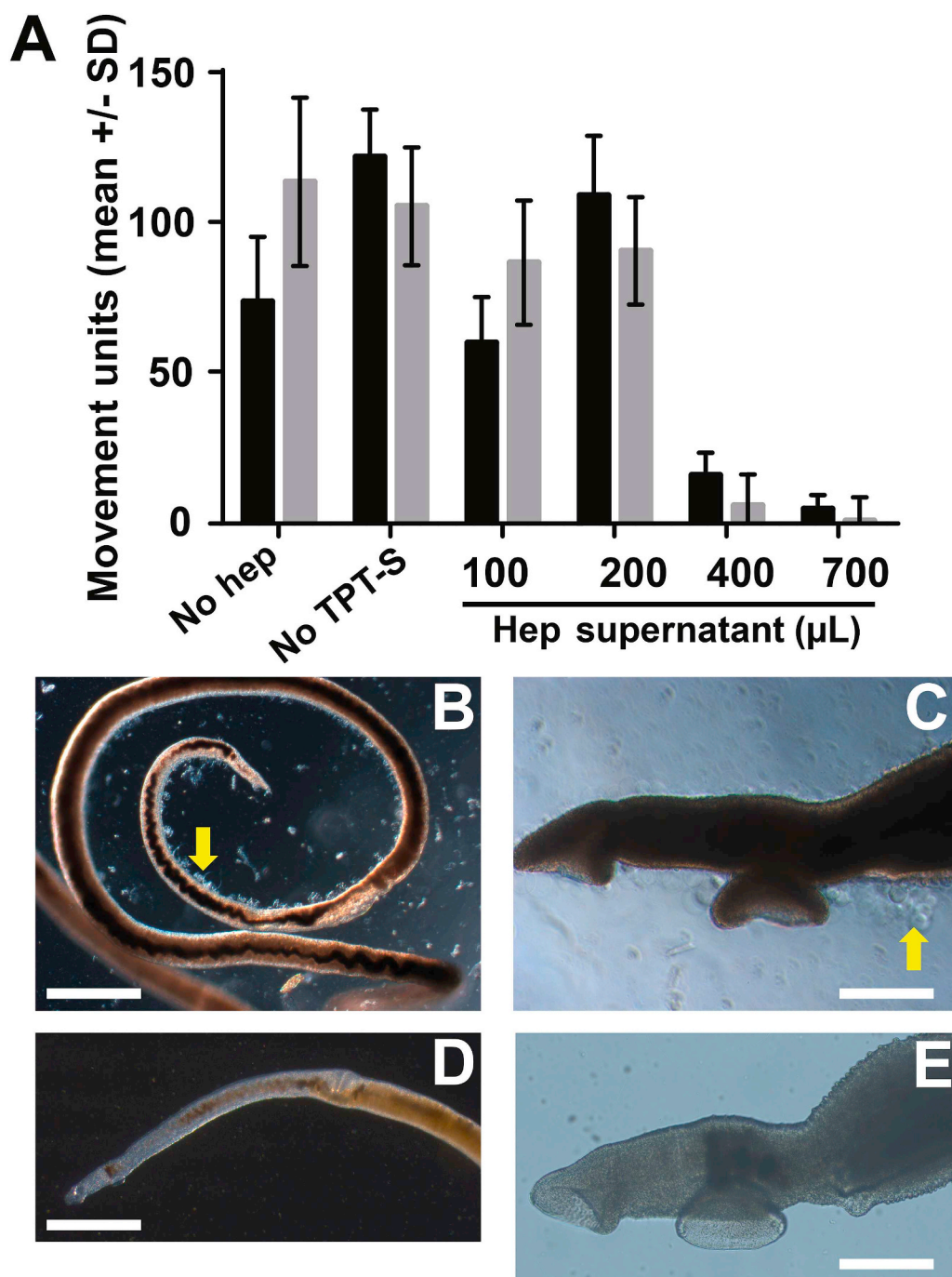


Fig. 7. Biotransformation of TPT sulfonate by hepatocytes is required for expression of anti-schistosomal activity *in vitro*. (A) Supernatants (100, 200, 400 or 700 µL) from rat hepatocytes that had been incubated with 750 µM TPT sulfonate for 30 min were added to 200 µL cultures of adult *S. mansoni*. Worm motility was measured with WormAssay after 2 h (black bars) and 18 h (grey bars). No hep. = a control whereby TPT sulfonate was incubated in hepatocyte medium but in the absence of hepatocytes before transfer of 700 µL of the medium to the parasites. No TPT-S = a control whereby hepatocytes had been incubated in the absence of TPT sulfonate before transfer of 700 µL of the medium to the parasites. The means ± SD values from one of two similar experiments are shown. (B) and (C) Images of worms incubated with 400 µL supernatant from rat hepatocytes that had been incubated with 750 µM TPT sulfonate for 30 min (B) A coiled female worm 18 h after incubation: the parasite's head is toward the center of view. (C) Anterior end of a male worm 18 h after a similar incubation: the oral sucker is to the left. For both images, arrows point to fraying and blebbing of the surface tegument. (D) and (E) Images of a female and male worm, respectively, incubated with 400 µL supernatant from rat hepatocytes that had been incubated in the absence of TPT sulfonate for 30 min. Bars represent 150 µm (B, D) and 50 µm (C, E), respectively.

3.9. Identification of TPT sulfonate metabolites observed in plasma and hepatocytes

Plasma from an initial mouse PK experiment (100 mg/kg PO) was analyzed to identify the metabolites of TPT sulfonate. The analysis was performed via neutral loss (NLS) and precursor ion scans (PIS) based on the major daughter ions of TPT sulfonate (m/z 234, 135, 120 and 91; Fig. 8A). The most useful technique proved to be m/z 56 NLS, employing the smallest neutral loss associated with the major daughter ions, which highlights compounds with a *t*-butyl group (Sassine et al., 2008), a moiety rare in biochemistry (Bisel et al., 2008). There is no single MS/MS scanning method that would detect all possible metabolites and m/z 56 NLS would not detect metabolites that are missing the *t*-butyl moiety or those with a modified *t*-butyl group. However, given the sensitive relationship between efficacy of TPT sulfonate

analogs and the structures of their *N*-alkyl substituents (with the *t*-butyl structure being associated with the greatest potency; see the R3 substituent in Table 1), it is less likely that metabolites lacking the *t*-butyl group contribute to efficacy. Moreover, the observed low rate of CYP oxidation of TPT sulfonate indicates that metabolites with modified *t*-butyl groups are unlikely to form. According to MetaSite, a software package that accurately predicts phase I metabolic transformations (Cruciani et al., 2013), the most abundant CYP-mediated modifications of TPT sulfonate, both overall and at the *t*-butyl moiety, should be hydroxylations. No such m/z 306 metabolites were detected either by the m/z 56 NLS (which would have detected phenyl modifications) or by the m/z 91, 120, 135 or 234 precursor ion scans (which would have detected *t*-butyl modifications). Thus, the *t*-butyl group is unlikely to be a site of metabolism and we expect that the m/z 56 NLS technique should detect the metabolites of most interest.

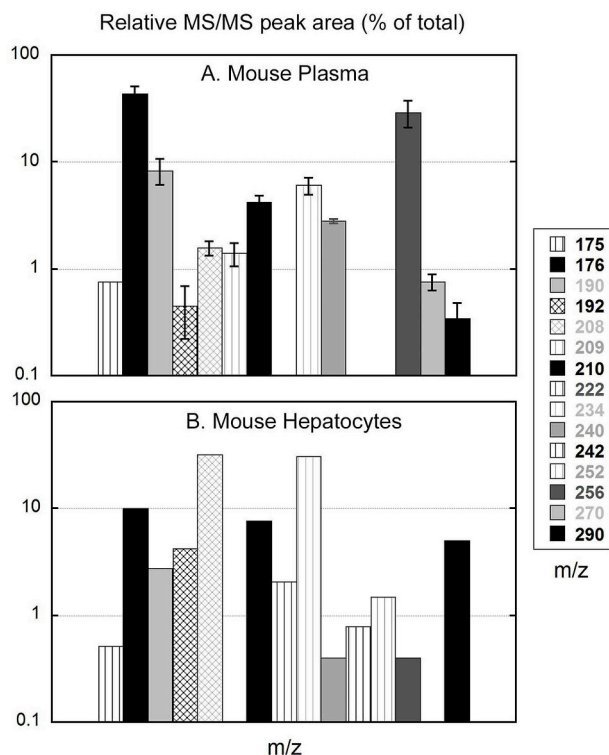


Fig. 8. Relative ion abundance of TPT sulfonate metabolites from mouse plasma and a mouse hepatocyte digest. MS/MS peak areas are compared for metabolites observed in (A) mouse plasma 4 h after 100 mg/kg PO dosing and in (B) a mouse hepatocyte incubation after 20 min, using 400 μ M TPT sulfonate and 3×10^6 cells/m. Solid colors represent metabolites depicted in Fig. 9; cross-hatching indicates metabolites differing from those in the figure by two mass units (possibly representing a gain or loss of a double bond) and vertical stripes indicate metabolites of unknown structure. Data were obtained via m/z 56 neutral loss scanning from m/z 100 to 320. The m/z 208 compound is not a metabolite *per se*, but a decomposition product that forms in the inlet to the API 4000 MS from the m/z 417 thiol dimer.

M/z 56 NLS of mouse plasma revealed over a dozen metabolites, as shown in Fig. 8A (a more complete list is presented in Table S2). The six prominent plasma metabolites moderately retained on a C8 column have m/z values of 176, 190, 210, 240, 256 and 270 (Figures S2 and S3). A striking feature of this list is that the m/z 176, 190 and 210 metabolites are related to the m/z 240 and 256 metabolites or to m/z 290 TPT sulfonate, respectively, by a mass loss of 80, a value diagnostic for loss of SO_3 . This made it straightforward to relate the structures of the first three metabolites with their immediate precursors and so reveal the major pathways of TPT sulfonate metabolism (Fig. 9). The m/z 256 and 270 precursors can be derived from the putative initially formed m/z 210 thiol metabolite via sequential oxidations. The plasma m/z 240 metabolite was deduced to be $\text{C}_{12}\text{H}_{18}\text{NS}_2$ on the basis of its observed (API 4000) MH^+ mass distribution (240.1, 100.0%; 241.1, 13.5%; 242.2, 9.5%, compared to the expected 240.09, 100.0%; 241.09, 13.0%; 242.08, 8.9%, as opposed to the values expected for $\text{C}_{12}\text{H}_{18}\text{NO}_2\text{S}$: 240.11, 100.0%; 241.11, 13.0%; 242.10, 4.4%). Dimerization of the m/z 210 thiol would be expected to form an m/z 417 disulfide, and the latter was found in plasma. Reduced glutathione was evidently either depleted or outcompeted in the location where the m/z 417 dimer formed. We also observed an m/z 208 peak that always eluted with the m/z 417 dimer, and, thus, appears to be a decomposition product of the dimer that forms in the API 4000 MS inlet. M/z 208, therefore, serves as a proxy for the dimer in the API 4000 m/z 56 NLS analyses.

Additional evidence to support our structural assignments was obtained from the MS and MS/MS analyses of a sample of the synthetic m/

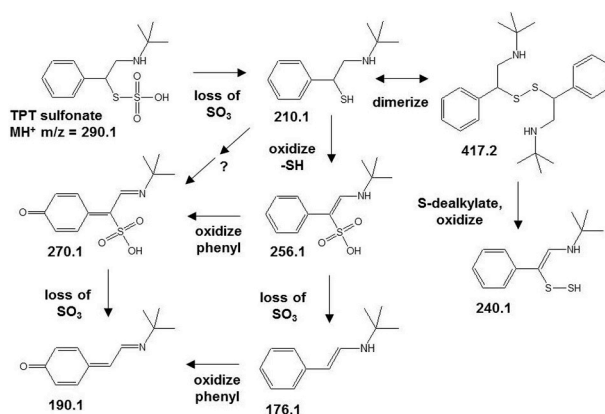


Fig. 9. Scheme of putative reactions that generate the major early-eluting metabolites of TPT sulfonate observed in mouse plasma. Sequential desulfations form three pairs of compounds with a mass difference of 80 (see Figures S2 and S3). All of these metabolites except the m/z 270 were also identified in hepatocyte incubations (Fig. 8B). Diagonal arrows represent a possible alternate pathway in which phenyl oxidation precedes sulphydryl oxidation.

z 417 thiol dimer (Figures S4 and S5). The absence of matrix in this sample allowed us to analyze it with a high mass resolution instrument, the LTQ Orbitrap. In the MS spectrum, we observed monomer and/or decomposition products with m/z values of 210 and 176, whereas in the MS/MS spectrum, we observed fragments with m/z 240, 210 and 176. In other words, species of the same mass as three of the TPT sulfonate plasma metabolites, representing all of the identified plasma metabolite structures with no added atoms other than hydrogen, formed from the sample. In addition, thiol dimer MS/MS fragments of m/z 208 and 242, representing species with the same masses as the putative API 4000 inlet decomposition product of the dimer and a putative hepatocyte metabolite, were also seen. The high accuracy mass values obtained allowed determination of the atomic compositions of each of these species. All of these results are consistent with the structures assigned to metabolites of the same mass.

Further evidence for the metabolite structures was obtained by analyzing mouse plasma samples using m/z 155 NLS and m/z 91, 120, 135 and 234 precursor ion scanning (PIS). Comparison of the putative metabolite structures in Fig. 9 and that of m/z 208 (see Figure S5) with the TPT sulfonate fragment structures in Fig. 8 indicates that the following detections should be impossible (because they require the loss of a fragment not contained within the metabolite structure): m/z 176 or 190 by m/z 135 PIS, any of the metabolites by m/z 234 PIS, and any except the m/z 256 or 270 by m/z 155 NLS. Of the 13 detections of one of these metabolites made using these methods, none fell into the forbidden category, consistent with our structural assignments.

The m/z 176 and 256 metabolites have the greatest ion abundances (based on MS/MS peak area) of those in plasma. Pure standards were not available for these analyses, and because MS/MS detection efficiency is variable, the actual molecular abundances are uncertain. Some of the additional metabolites (Table S2) differ from those shown in Fig. 9, by the mass of a double bond, whereas others have no obvious relation to the known structures; the most prominent of the latter are the late-eluting m/z 234 and 209 (Figure S3).

A plot of the relative peak size of mouse plasma metabolites from 0.5 to 4.0 h after PO dosing does not show strong trends during that interval in most cases (Figure S6). The only metabolites to show a large (> 3-fold) and statistically significant increase over this interval were the m/z 190 ($p = 0.04$) and 270 ($p = 0.01$) quinone methides, suggesting that the oxidation of the phenyl moiety is slow relative to the other biotransformations. Possible reasons for this outcome, beyond simple formation kinetics, are that quinone methide formation is less favored in the first pass or that this pathway is upregulated after dosing; these metabolites might also have longer half-lives than the others. The

Table 3
Non-compartmental mouse pharmacokinetics of TPT sulfonate.

	IV (15 mg/kg)		PO (100 mg/kg)	
	$t = 0 \rightarrow \text{last}$	$t = 0 \rightarrow \infty$	$t = 0 \rightarrow \text{last}$	$t = 0 \rightarrow \infty$
C_o (ng/ml)	37,200	–	–	–
C_{max} (ng/ml)	–	–	710	–
V_o (l/kg)	0.403	–	–	–
V_{ss} (l/kg)	0.693	0.984	–	–
V_{area} (l/kg)	7.9 ^a	7.7 ^a	7.9 ^a	7.7 ^a
CL (ml/min/kg)	99.6	97.6	–	–
AUC (ng·h/ml)	2510	2560	1430	1450
MRT [+ MIT] (h)	0.116	0.168	[1.83]	[1.94]
F (%)	–	–	–	8.5

Abbreviations: V_o , time zero volume of distribution = dose/C_o ; V_{ss} , steady-state volume of distribution = $CL \cdot MRT$; V_{area} , terminal volume of distribution = $CL / \text{terminal } k$; CL , plasma clearance; AUC , area under the plasma concentration-time curve; MRT , mean residence time; MIT , mean input time; F , bioavailability.

^a Based on the IV CL and the average of the k values from the last three data points of the IV and PO PK datasets (see Section 3.10).

analyte displaying the most significant downward trend (decreasing more than 50% in the same interval) was the m/z 290 parent drug ($p = 0.07$).

Of the major ($> 0.7\%$ abundance) metabolites initially observed in mouse plasma, all but the m/z 209 and m/z 270 products were also observed in mouse hepatocyte digests (Fig. 8B; Table S2) along with the m/z 417 disulfide of the m/z 210 thiol. With the hepatocytes, there is a higher initial TPT sulfonate concentration than in the plasma, leading to a higher early concentration of thiol (represented by m/z 210 and m/z 208 from the dimer). This intermediate might have saturated the pathway leading to m/z 256 and its downstream m/z 176, 270 and 190 metabolites, resulting in relatively less of these, and relatively more of the metabolites from other pathways, e.g., m/z 222, 234, and 252. The hepatocyte metabolites analyzed include those extracted from within cells.

3.10. Full mouse PK experiment (IV/PO)

A PK study of TPT sulfonate following IV and PO dosing of mice indicates that its bioavailability (F) is about 8.5% (Table 3). The plasma clearance value of almost 100 ml/min/kg approximates the rate of mouse hepatic blood flow of 90 ml/min/kg; (Davies and Morris, 1993), indicating that TPT sulfonate is rapidly cleared. Based on the AUC , the mean residence time is approximately 10 min for the IV data and, including mean input time, almost 2 h for the PO data (Table 3). The rapid metabolism relative to the absorption rate implies flip-flop kinetics, i.e., the terminal elimination rate after oral dosing may be controlled by absorption. The mean PO/IV ratio of metabolite AUC s, normalized to dose, was 1.03 (Table 4). This indicates that TPT

sulfonate is fully absorbed and that its low bioavailability is due to extensive ($\geq 90\%$) first-pass metabolism.

The apparent plasma half-life of TPT sulfonate (calculated from the last three time points in Fig. 10A) was 1.3 h from the PO data and 0.7 h from the IV data. These values are significantly shorter than those of its metabolites, consistent with its role as a prodrug (Table 4). The natural log of plasma concentration vs. time plot for the PO data reaches a linear terminal phase ($R = 0.995$). However, the corresponding IV data is decidedly nonlinear ($R = 0.81$) with half-lives calculated from adjacent time point pairs starting at 0.04 h and then increasing to over an hour. The progression indicates that after IV dosing, TPT sulfonate distributes out of the central compartment into other tissues, becoming less subject to hepatic elimination as it does so. Reflecting this migration, the volume of distribution increases from an initial IV value of 0.4 L/kg to a final value of ~ 8 L/kg (Table 3). The apparent PO half-life represents an upper limit for the true terminal plasma half-life, due to slow GI absorption, whereas the IV value is probably a lower limit since it doesn't attain a linear phase.

The m/z 210 thiol metabolite had by far the shortest t_{max} after IV dosing (Table 4, Fig. 10B), consistent with it being the first metabolite to form. However, its t_{max} with PO dosing was among the longest. In addition, its PO terminal half-life of 6 h was longer than those of the downstream metabolites analyzed. The larger TPT sulfonate dose given PO may have led to a greater proportion of thiol dimer formation. Reversible heterodisulfide formation by the thiol is also likely, but, at least initially, probably to a lesser extent than homodisulfide formation. Formation of both types of disulfides probably protects the thiol from further metabolism. Gradual reduction of the additional dimer back to thiol monomer could then explain the latter's longer PO t_{max} . The longer plasma half-life of the thiol relative to the other metabolites may reflect that once released into plasma it is less subject to reuptake by the liver for further metabolism.

The kinetics of formation and elimination of the m/z 256 alkenyl sulfonic acid were generally similar to those of the m/z 176 styrene metabolite (Table 4; Fig. 10C, D) consistent with formation of the latter via sequential metabolism, i.e., m/z 256 formation rate-limits m/z 176 formation. Both have t_{max} values in the 0.5–1.0 h range after IV administration and close to 3 h after PO dosing, and terminal half-lives of about 2 h. The apparent relatively greater AUC of m/z 256 when dosed PO may reflect a different selectivity for metabolite formation in the first pass.

A puzzling aspect of the m/z 176 metabolite is that, whereas only one peak was seen for this molecular weight in our initial mouse PK study (Figure S3C), three peaks were seen in the final study (utilizing a different chromatographic system; Fig. 10D). These peaks could not be distinguished from one another on the basis of parent ion m/z (using NLS) or daughter ion m/z (using a product ion scan). The two main peaks (at 0.66 and 0.79 min) had very similar plasma time profiles (Table 4; Fig. 10D). Several isomeric or stereoisomeric structures are possible for the metabolite and one explanation is that they might have

Table 4
Non-compartmental mouse pharmacokinetics of TPT sulfonate and its metabolites.

Chemical species	t_{max} (h)		terminal $t_{1/2}$ (h)		AUC ratio, PO/IV (normalized to dose)
	IV	PO	IV	PO	
TPT sulfonate (m/z 290)	–	0.50	–	1.3 ^b	0.085 ^a
m/z 210	0.083	4.0	–	5.8 ^b	0.84 ^c
m/z 256	1.0	2.0	2.2 ^b	2.5 ^b	1.49 ^c
m/z 176, 0.79 min peak	0.5	2.0	1.7 ^b	2.4 ^b	0.98 ^c
m/z 176, 0.66 min peak	0.5	4.0	1.7 ^b	2.3 ^b	1.05 ^c
m/z 176, 1.25 min peak	0.5	2.0	–	1.6 ^b	0.81 ^c

^a From WinNonlin analysis for $t = 0 \rightarrow \infty$

^b From slope of last 3 data points of \ln peak area vs. time plot, for cases with $R > 0.98$.

^c From AUC_{0-8h} ; mean value for metabolites is 1.03 ± 0.27 .

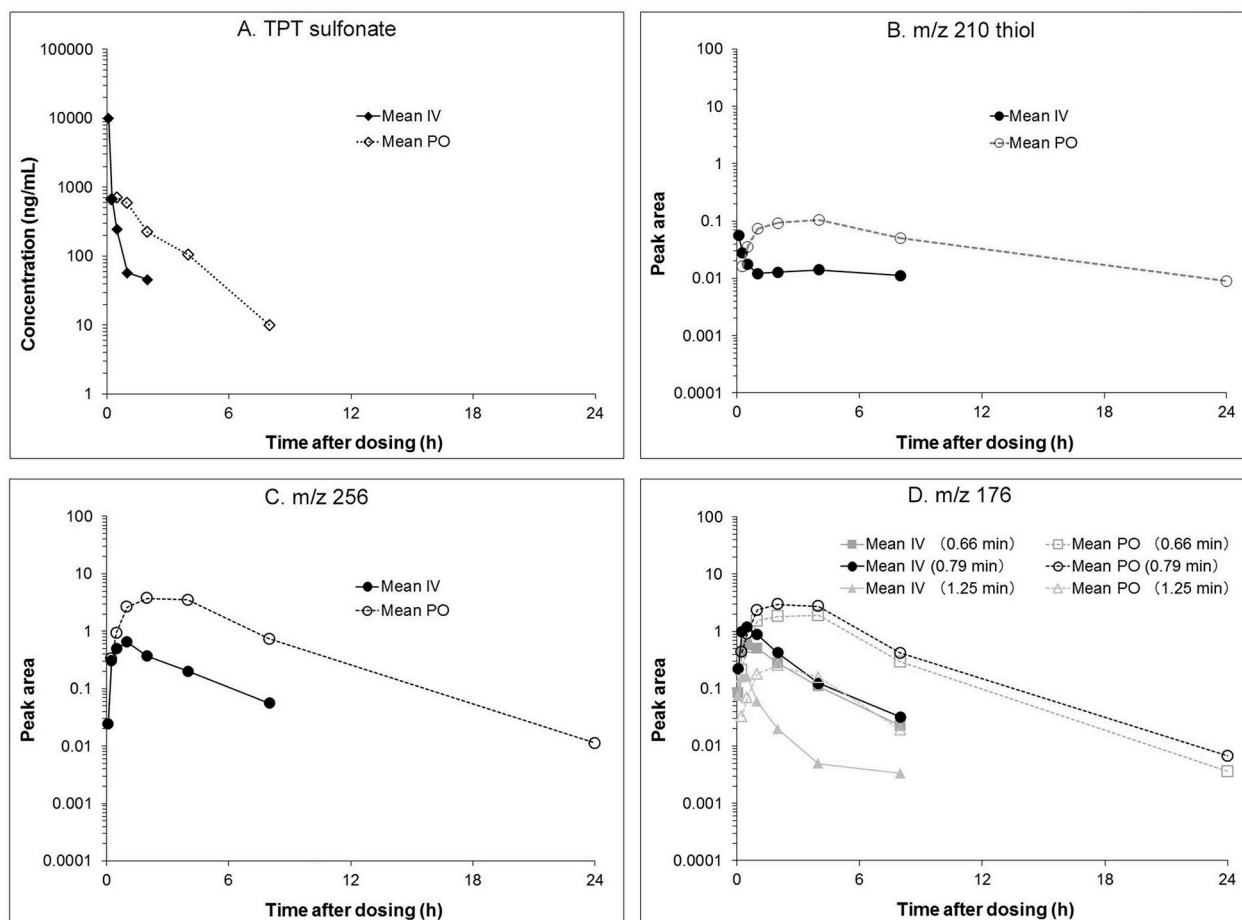
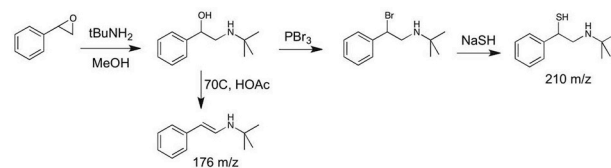


Fig. 10. Plasma-time profiles of TPT sulfonate and three of its metabolites in mice after IV and oral dosing. Mice were administered TPT sulfonate IV (4 mice, 15 mg/kg) or PO (8 mice, 100 mg/kg), as described in the Materials and Methods. Mean TPT sulfonate plasma concentrations and metabolite MS/MS peak areas were then determined. (A) TPT sulfonate (retention time = 1.14 min). (B) The m/z 210 thiol metabolite initially formed from desulfation of TPT sulfonate (retention time = 1.10 min). (C) The m/z 256 alkenyl sulfonic acid metabolite formed by oxidation of the m/z 210 thiol (retention time = 0.82 min). (D) The m/z 176 2-phenylethanamine metabolite(s) formed by desulfation of the m/z 256 metabolite. Three retention times were observed for the m/z 176 metabolite, whereas in our original mouse PK study this m/z was represented by a single peak (see Figure S3C and Discussion). Note: these retentions are from a different LC method than those in shown in Figure S2 and Figure S3.

co-eluted under our initial but not our final analytical conditions due to different rates of interconversion. Alternatively, multiple metabolites might exist that decompose into an m/z 176 ion in the mass spectrometer inlet only under the conditions employed in the second (full) PK study. In our initial study, we observed inlet decomposition of the m/z 417 thiol dimer into m/z 208 and 224. In later work under different conditions, we sometimes also observed other inlet decompositions, such as 417 to 361, 417 to 242, 290 to 210 and 224 to 176. Which chromatographic and/or detection system variables influenced this process are not clear. Although inlet decomposition of m/z 240 to m/z 176 was evident in the final PK study, this fact did not account for any of the m/z 176 peaks we analyzed.

3.11. *In vitro* identification of the m/z 210 thiol metabolite (TP thiol) as a cidal principle with low cell toxicity

Mouse metabolism of TPT sulfonate generates the m/z 210 thiol in the initial step (Fig. 9), whereas the m/z 176 styrene is the metabolite observed to have the largest LC-MS/MS peak area (a proxy for abundance in the absence of weighed standards or a radiolabel). Both of these metabolites also form in the transformation of TPT sulfonate by hepatocytes *in vitro* (Fig. 9, Table S2). Accordingly, they were synthesized by the CRO WuXi using a synthetic scheme designed by us



Scheme 1. Synthesis of m/z 210 thiol (TPT thiol) and 176 styrene metabolites.

(Scheme 1): synthesis of the m/z 210 component (TP thiol) yielded the m/z 417 dimer due to spontaneous disulfide bond formation upon concentration of the reaction mixture.

After 8 h, TP thiol generated a concentration-dependent decrease in motility of both adult *S. mansoni* and *S. haematobium* (Fig. 11A). The principal microscopic observations were markedly decreased movement, an inability of the worms to adhere to the well floor and the sexes becoming uncoupled. In contrast, the m/z 176 styrene was inactive against both schistosome species up to 40 μ M after 24 h. In 24 h counter-toxicity screens with three mammalian cell lines, the TP thiol was relatively non-toxic up to the highest concentration tested of 40 μ M, at which concentration cell nuclei counts were decreased to 86, 78 and 100% of DMSO controls for C2C12, HuH-7 and BESM cells, respectively (Fig. 11B).

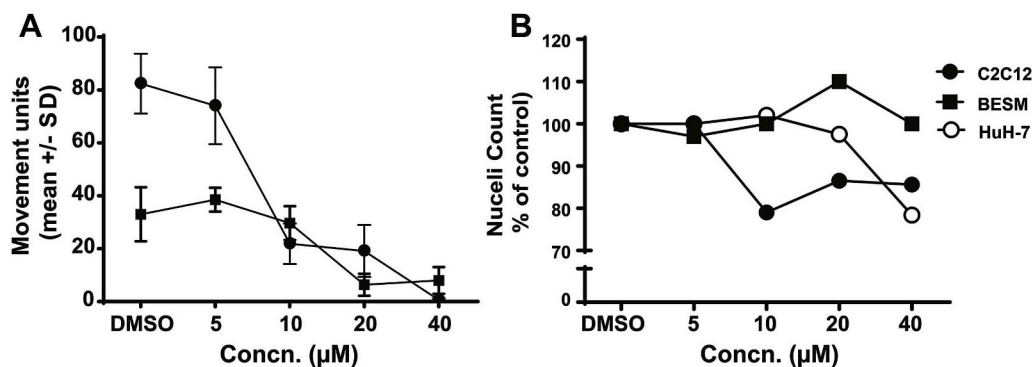


Fig. 11. *In vitro* bioactivity of the chemically synthesized m/z 210 metabolite (TP thiol) against adult *S. mansoni* and *S. haematobium*, and apparent lack of cell toxicity. (A) Adult *S. mansoni* (circles) or *S. haematobium* (squares) were incubated for 8 h with different concentrations of synthesized TP thiol (as the m/z 417 dimer). Points represent the means \pm SD values across three wells at each concentration and one of two experiments is shown. (B) Counter toxicity screens with various mammalian cell lines incubated in the presence of TP thiol were performed as shown.

described in the Materials and Methods. After 24 h, cells were fixed with 10% paraformaldehyde and nuclei stained with DAPI. Nuclei were counted across 5–10 fields of view/well using an inverted microscope fitted with a 20x objective lens. Nuclei counts are expressed as percentages relative to DMSO controls. Points represent mean counts across a minimum of three wells for each concentration tested and the S.D. value for each mean was $\leq 20\%$. Data from one of two experiments performed are shown.

3.12. Chemically synthesized TP thiol is parasitocidal *in vivo*

Sufficient TP thiol (as the corresponding dimer) had been synthesized by WuXi to administer a single 50 mg/kg dose IP in 2.5% Kolliphor EL to mice harboring 33-day-old infections. Female and male worm burdens were decreased by 35% and 44% in one experiment, respectively (Table S1 worksheet 18). All of the worms recovered were approximately 50% less massive and paler relative to vehicle controls. Also, infection-related organomegaly was decreased: liver and spleen weights were 32% and 41% lower compared to those of the vehicle controls.

4. Discussion

With the continuing international resolve to make PZQ available to more communities affected by schistosomiasis, there is concern that sufficient drug pressure will eventually lead to parasites exhibiting reversible or, worse, genetically fixed resistance. In addition, there is a need to provide a drug that does not suffer the pharmacological weaknesses of PZQ, chief among which are its lack of cure in the single dose typically offered and its incomplete efficacy against the parasite, in particular against 21–28-day-old juvenile worms (Gönnert and Andrews, 1977; Sabah et al., 1986; Keiser et al., 2009).

As possible alternatives to PZQ, Pellegrino, and then Nelson and colleagues have shown that aliphatic or phenyl-substituted aminoalk-anethiosulfates kill *S. mansoni* in a mouse model of infection. Apart from one study (Penido et al., 1994) with one of the 15 compounds tested here (compound 8 see below), the emphasis has been on targeting adult worms (Nelson and Pellegrino, 1976; Penido et al., 1994; Moreira et al., 2007) and the potential efficacy of this compound series against younger stages of the parasite, including those 21–28 day-old parasites most refractory to PZQ, has not been investigated. Here, using an initial screening dose of 100 mg/kg PO QDx4, we found that three of the 15 thiosulfates tested (compounds 1, 2 and 8) significantly reduced the burdens of 42-day-old adult and 21-day-old juvenile *S. mansoni* in mice. The greater efficacy against mature female worms noted here is consistent with previous data for these and other thiosulfates (Penido et al., 1994, 1995, 1999; Moreira et al., 2007) and is extended here to include females from immature infections.

Examination of the *in vivo* structural-bioactivity data suggests that phenyl substitution adjacent to the sulfur of the thiosulfate is associated with more active compounds (in the 15-member series, the 4 phenyl-bearing representatives include the 3 most active compounds at 21 dpi). The identification of active metabolites derived from 2 (see below) raises the possibility that the SAR observed for this series might be complicated by a structural effect on the rate of host metabolism in addition to the influence of structure on the parasite interaction. Also,

we have not tested the possibility that thiosulfates which lack *in vivo* efficacy may generate hepatocyte metabolites with *in vitro* anti-schistosomal activity.

The most effective compound to emerge from the initial 100 mg/kg QD x4 screen was compound 2, TPT sulfonate. TPT sulfonate does not violate any of the guidelines for drug-like molecules put forward by Lipinski et al. (2001) or Veber et al. (2002). At single oral doses, the compound was superior to PZQ against 21-day-old juvenile parasites; 80–90% worm-kill was measured compared to zero kill for PZQ. Against adult 42-day-old worms at 400 mg/kg, TPT sulfonate was competitive with PZQ with reductions of 100% and approximately 80% for female and male worm burdens, respectively, compared to 100% for both sexes with PZQ. No further worm burden reductions were achieved at the higher dose of 600 mg/kg TPT sulfonate.

The efficacy of TPT sulfonate also extended to 11- and 15-day-old juveniles that have completed their migration across the lungs and taken up residency in the mesenteric venous system (Rheinberg et al.). However, younger parasites (1-day-old skin larvae and 7-day-old lung-stage worms) were more resilient. In the case of the lung-stage worms, twice the initial screening dose, i.e., 200 mg/kg QDx4 was needed to demonstrate a significant cidal affect. The difference in susceptibility between skin-/lung-stage somules and juvenile worms in the mesenteric veins was noted before for one compound (8) whereby a 300 mg/kg QDx5 dose was 50% efficacious against 24 day-old *S. mansoni* but ineffective against the parasites 1–10 dpi (Penido et al., 1994). The reason for the apparent resilience of skin-/lung-stage worms is unclear but may lie in the nature of the parasites themselves (e.g., poorer penetration of the active principle or altered expression of the target(s)) and/or the availability of the active principle in the relevant tissues.

Compared to the often robust cidal activity measured *in vivo*, none of the 15 sulfonates was active against parasites *in vitro* (somules or adults) at concentrations of up to 10 μM over 3 days. The result essentially made an *in vitro*-based development of an SAR impossible. Previous *in vitro* tests using *S. mansoni* adults, newly transformed and six-day-old lung-stage stage somules with compounds 5, 6, 8, 10, and 13 noted paralysis and tegumental damage for some of the compounds tested (Penido et al., 1994). However, the studies employed very high compound concentrations (0.25–1 mM) and the physiological relevance of the changes reported is unclear. The absence of activity in our *in vitro* assays suggested a prodrug mechanism of action, a notion substantiated for TPT sulfonate by the finding that supernatants from rat hepatocytes that had been incubated with the compound markedly decreased the motility of adult *S. mansoni* and *S. haematobium* and induced degenerative changes.

Although TPT sulfonate was readily biotransformed by whole hepatocytes from either mice or rats, it was not oxidized or glucuronidated by isolated mouse liver microsomes. These findings suggest

that metabolic clearance pathways are independent of the two most common classes of drug-metabolizing enzymes, a desirable feature that decreases the likelihood of problematic drug-drug interactions, particularly because the current drug, PZQ, is dispensed to populations with minimal medical supervision. About a dozen CYP isoforms metabolize 70–80% of all drugs (Zanger and Schwab, 2013) and UGTs are the most prominent conjugating enzymes in drug metabolism. Together, CYPs and UGTs account for over 90% of hepatic drug metabolism (Rowland et al., 2013). For TPT sulfonate, the cytosolic enzymes, aldehyde oxidase and various carboxylesterases might contribute to its conversion to the active thiol form: sulfatases could also be involved (Coughtrie et al., 1998; Bojarova and Williams, 2008). Given the broad similarities in hepatic metabolism across mammals, it is likely that human hepatocytes will metabolize TPT sulfonate similarly to rodent hepatocytes. However, confirming this and identifying the enzyme(s) involved will require further work.

Based on the full mouse PK (IV/PO) study, TPT sulfonate appears to be fully absorbed when administered orally and is rapidly metabolized by the liver with over 90% being metabolized in the first pass. To identify TPT sulfonate metabolite(s), NLS MS/MS analysis was performed with mouse plasma samples taken at various time points up to 4 h post oral dosing and with supernatants withdrawn from rat hepatocytes incubated with TPT sulfonate for up to 30 min. Eight major plasma metabolites (each with over 1% of total metabolite MS/MS peak area) were found (Fig. 8) and structures were identified for six of these (Fig. 9). Seven of the eight were also found in hepatocyte digests (Fig. 8).

The *m/z* 210 thiol (TP thiol) and 176 styrene metabolites were selected for synthesis and activity-testing against the parasite *in vitro*. They were chosen because the *m/z* 210 is the first metabolite formed in the metabolism scheme, and, thus, would be capable of generating all downstream metabolites, whereas the *m/z* 176 appears to be most abundant metabolite. Activity (decreased motility) was only demonstrated for the TP thiol, a finding that extended to *S. haematobium* which is often co-endemic with *S. mansoni* in Africa. The finding is important as the current drug, PZQ, is active against all medically relevant schistosomes. Furthermore, after IP administration, TP thiol was active *in vivo*, significantly reducing the male worm burden, a result that is in line with TP thiol's long plasma half-life (approximately 6 h) in mice which would favor elimination of the parasite. The *in vivo* generation of TP thiol is consistent with the earlier identification of a major disulfide metabolite after oral administration of 2-(*sec*-butylamino)-1-octanethiosulfuric acid to mice infected with *S. mansoni* (Penido et al., 1995), although cidal activity was not directly linked to the particular metabolite at that time. Even though TP thiol is isolated as a disulfide dimer upon chemical synthesis, it would be reduced back to the thiol monomer under most intracellular conditions (Fig. 9, Table S2). The *in vitro* anti-schistosomal activity of TP thiol demonstrates that the parasite might not be able to desulfate the TPT sulfonate parent drug, but does not make clear whether the thiol is ultimately the active schistosomicide because the parasite's ability to metabolize it further has not been determined.

Looking forward, the identification of a parasitocidal metabolite is significant as it not only facilitates an understanding of the chemistry supporting the bioactivity but also allows the convenient *in vitro* assessment of anti-parasite activity and identification of the mechanism of action and/or target. The known susceptibility of the schistosome to perturbation in redox conditions, including depletion of glutathione levels (Bueding et al., 1982; Mkoji et al., 1990; Williams et al., 2013), might be a good match for this prodrug's ability to form metabolites with both oxidative (quinone methides) and reductive (a thiol and conjugated phenyls) potential, and the capacity to mop up GSH in a heterodisulfide. We are currently investigating the possible effects on redox by TP thiol, including whether GSH levels are depleted in the worm.

TP thiol is a free thiol putatively formed by cleavage of the

thiosulfuric acid group of the TPT sulfonate. The mechanisms by which the active product is generated are not yet clear. Free sulfhydryl groups are generally disliked in pharmaceutical development (Jaffe, 1986) and are used much less than amino, hydroxyl or carboxylic acid functional groups (Carey et al., 2006). They can form protein adducts, often by displacing a cysteine from a cysteine disulfide residue, as well as other types of disulfides; thus, their toxicity is increased by GSH depletion. They can also potentially be oxidized to more reactive sulfenic acid and sulfinic acid metabolites (Kalgutkar et al., 2005). Complications arising from non-selective off-target alkylations can confound *in vivo* experiments unless appropriate controls are in place. In our hands, however, up to 40 μ M TP thiol demonstrated little toxicity toward three different mammalian cell lines after 24 h. Furthermore, the presence of a free thiol *per se* is not an impediment to successful drug development and there are a number of marketed drugs used for chronic conditions that bear a free thiol group. These include the angiotensin-converting enzyme (ACE) inhibitors, captopril and zofenopril (the latter a pro-drug that is de-esterified to the active inhibitor, zofenoprilat), thiorphan, which is the active metabolite of the antidiarrheal racecadotril (acetorphan), and tiopronin, which is used primarily for cystinuria. In mice, these free-thiol drugs are essentially non-toxic in single oral dose tolerability tests with LD₅₀ values > 2 g/kg (Imai et al., 1981; Challener, 2001) (<http://www.drugfuture.com/toxic/q60-q161.html>). Finally, an erstwhile drug for schistosomiasis, Oltipraz, also contains a free thiol and has found new life as an antisteatotic agent whereby oral doses of 60 mg/*BID* over 24 weeks were well-tolerated in a recent randomized clinical trial (Kim et al., 2017) (www.clinicaltrials.gov: NCT01373554).

A second type of reactive structure, the quinone methide, is present in the *m/z* 190 and 270 metabolites of TPT sulfonate. Quinone methides are electrophiles and may react with glutathione and protein thiol groups (Monks and Jones, 2002) or DNA (Wang et al., 2005). Drugs that have quinone methide structures or which generate quinone methide metabolites include the anti-estrogens (such as tamoxifen and raloxifene) which are used in cancer treatment (Kalgutkar et al., 2005). Some natural products and food additives, e.g., quercetin and butylated hydroxytoluene (BHT), are also metabolized to quinone methides (Dufrasne et al., 2011). Given that some of the drugs associated with these metabolites can be dosed for periods of years, the possible hazards of a brief exposure during acute treatment for schistosomiasis are not clear.

A basic target profile has been suggested for new anti-schistosomal drugs (Nwaka and Hudson, 2006; Caffrey, 2007) into which the current compound, TPT sulfonate, fits reasonably well. Among the pharmacological criteria discussed, the compound should: (i) be active against all major schistosome species infecting humans; (ii) be active against immature flukes against which PZQ has little or no activity; (iii) be orally active, preferably as a single dose; (iv) belong to a different chemical class than PZQ; and (v) possess a mechanism of action different from that of PZQ. Although the last point has yet to be clarified, we might anticipate a different mechanism of action based on the quite different chemistries and the gross phenotypic responses of the parasite *in vitro* to the TP thiol (appearance of 'flaccid-paralysis') and PZQ (tetanic or constricted paralysis; (Andrews et al., 1983; Andrews, 1985; Pica-Mattoccia and Cioli, 2004; Abdulla et al., 2009). Attractive attributes of TPT sulfonate are (i) ease of synthesis which is accomplished in three to four steps using low-cost reagents and an overall yield of approximately 40%; and (ii) cost, whereby the reagents and solvents necessary for the laboratory-scale synthesis of 10 mol (2890 g) of TPT sulfonate cost US\$ 1800.00. If bulk quantities of the reagents are used, the overall cost of the product would likely be lower.

In regard of the pursuit of TPT sulfonate/TP thiol as a possible lead anti-schistosomal, factors for further investigation, apart from defining the mechanism of action discussed above, include the influence of chirality on anti-parasite activity and the chemical modification of the TP thiol scaffold to improve potency and drug-like properties. Among the alterations being considered is a replacement and/or deletion of the

thiol to formally confirm its requirement for anti-parasite activity and, if needed, for modified scaffolds. Also, constraining the central portion of the molecule by incorporating a heterocycle would conceivably increase the *in vivo* stability of active forms.

5. Conclusions

From 15 S-[2-(alkylamino)alkane] thiosulfuric acids that were profiled in mice for oral efficacy against both mature and developing *Schistosoma mansoni*, TPT sulfonate emerged as the most effective in decreasing worm burdens. The efficacy spectrum determined is competitive with that of PZQ. TP sulfonate must be biotransformed to reveal its anti-schistosomal activity. In mice, TPT sulfonate is fully absorbed and subject to rapid, non-CYP-mediated, first-pass metabolism. The first of many metabolites produced, namely TP thiol, was synthesized and shown to possess anti-schistosomal activity both *in vitro* and *in vivo*. Investigations to understand TP thiol's mechanism(s) of action and/or target are ongoing, as are efforts to improve its chemistry.

Conflicts of interest

The authors declared that there is no conflict of interest.

Acknowledgements

We thank Juan C. Engel for advice regarding the counter-toxicity screening experiments. D. L. Nelson was the recipient of a PVNS fellowship from the Coordenação do Aperfeiçoamento de Pessoal de Ensino Superior (CAPES). The research reported was supported by a UCSF Clinical Translational Science Institute T1 Catalyst Award, and the NIH-NIAID R01AI089896 and R21AI107390 awards.

Appendix A. Supplementary data

Supplementary data to this article can be found online at <https://doi.org/10.1016/j.ijpddr.2018.10.004>.

References

- Abdulla, M.H., Lim, K.C., Sajid, M., McKerrow, J.H., Caffrey, C.R., 2007. Schistosomiasis mansoni: novel chemotherapy using a cysteine protease inhibitor. *PLoS Med.* 4 e14.
- Abdulla, M.H., Ruelas, D.S., Wolff, B., Snedecor, J., Lim, K.C., Xu, F., Renslo, A.R., Williams, J., McKerrow, J.H., Caffrey, C.R., 2009. Drug discovery for schistosomiasis: hit and lead compounds identified in a library of known drugs by medium-throughput phenotypic screening. *PLoS Neglected Trop. Dis.* 3, e478.
- Andrews, P., 1985. Praziquantel: mechanisms of anti-schistosomal activity. *Pharmacol. Ther.* 29, 129–156.
- Andrews, P., Thomas, H., Pohlke, R., Seubert, J., 1983. Praziquantel. *Med Res Rev* 3, 147–200.
- Basch, P.F., 1981. Cultivation of *Schistosoma mansoni* in vitro. I. Establishment of cultures from cercariae and development until pairing. *J. Parasitol.* 67, 179–185.
- Bisel, P., Al-Momani, L., Muller, M., 2008. The tert-butyl group in chemistry and biology. *Org. Biomol. Chem.* 6, 2655–2665.
- Blau, H.M., Pavlath, G.K., Hardeman, E.C., Chiu, C.P., Silberstein, L., Webster, S.G., Miller, S.C., Webster, C., 1985. Plasticity of the differentiated state. *Science* 230, 758–766.
- Bojarova, P., Williams, S.J., 2008. Sulfotransferases, sulfatases and formylglycine-generating enzymes: a sulfation fascination. *Curr. Opin. Chem. Biol.* 12, 573–581.
- Botros, S., Pica-Mattoccia, L., William, S., El-Lakkani, N., Cioli, D., 2005. Effect of praziquantel on the immature stages of *Schistosoma haematobium*. *Int. J. Parasitol.* 35, 1453–1457.
- Brindley, P.J., Sher, A., 1987. The chemotherapeutic effect of praziquantel against *Schistosoma mansoni* is dependent on host antibody response. *J. Immunol.* 139, 215–220.
- Bueding, E., Dolan, P., Leroy, J.P., 1982. The antischistosomal activity of oltipraz. *Res. Commun. Chem. Pathol. Pharmacol.* 37, 293–303.
- Caffrey, C.R., 2007. Chemotherapy of schistosomiasis: present and future. *Curr. Opin. Chem. Biol.* 11, 433–439.
- Caffrey, C.R., 2015. Schistosomiasis and its treatment. *Future Med. Chem.* 7, 675–676.
- Carey, J.S., Laffan, D., Thomson, C., Williams, M.T., 2006. Analysis of the reactions used for the preparation of drug candidate molecules. *Org. Biomol. Chem.* 4, 2337–2347.
- Challenger, C., 2001. *Chiral Drugs*. Ashgate Publishing Ltd., Aldershot, UK.
- Colley, D.G., Bustinduy, A.L., Secor, W.E., King, C.H., 2014. Human schistosomiasis. *Lancet* 383, 2253–2264.
- Colley, D.G., Wikel, S.K., 1974. *Schistosoma mansoni*: simplified method for the production of schistosomules. *Exp. Parasitol.* 35, 44–51.
- Coughtrie, M.W., Sharp, S., Maxwell, K., Innes, N.P., 1998. Biology and function of the reversible sulfation pathway catalysed by human sulfotransferases and sulfatases. *Chem. Biol. Interact.* 109, 3–27.
- Cruciani, G., Baroni, M., Benedetti, P., Goracci, L., Fortuna, C.G., 2013. Exposition and reactivity optimization to predict sites of metabolism in chemicals. *Drug Discov. Today Technol.* 10, e155–165.
- Cruciani, G., Crivori, P., Carrupt, P.-A., Testa, B., 2000a. Molecular fields in quantitative structure–permeation relationships: the VolSurf approach. *J. Mol. Struct.: Theorchem* 503, 17–30.
- Cruciani, G., Pastor, M., Guba, W., 2000b. VolSurf: a new tool for the pharmacokinetic optimization of lead compounds. *Eur. J. Pharmaceut. Sci.: Official J. Eur. Fed. Pharmaceut. Sci.* 11 (Suppl. 2), S29–S39.
- Davies, B., Morris, T., 1993. Physiological parameters in laboratory animals and humans. *Pharm. Res. (N. Y.)* 10, 1093–1095.
- de Oliveira Penido, M.L., Zech Coelho, P.M., de Mello, R.T., Pilo-Veloso, D., de Oliveira, M.C., Kusel, J.R., Nelson, D.L., 2008. Antischistosomal activity of aminoalkanethiols, aminoalkanethiosulfuric acids and the corresponding disulfides. *Acta Trop.* 108, 249–255.
- Doenhoff, M.J., Sabah, A.A., Fletcher, C., Webbe, G., Bain, J., 1987. Evidence for an immune-dependent action of praziquantel on *Schistosoma mansoni* in mice. *Trans. R. Soc. Trop. Med. Hyg.* 81, 947–951.
- Dufresne, F., Gelbcke, M., Neve, J., Kiss, R., Kraus, J.L., 2011. Quinone methides and their prodrugs: a subtle equilibrium between cancer promotion, prevention, and cure. *Curr. Med. Chem.* 18, 3995–4011.
- Duvall, R.H., DeWitt, W.B., 1967. An improved perfusion technique for recovering adult schistosomes from laboratory animals. *Am. J. Trop. Med. Hyg.* 16, 483–486.
- Engel, J.C., Doyle, P.S., Dvorak, J.A., 1985. *Trypanosoma cruzi*: biological characterization of clones derived from chronic chagasic patients. II. Quantitative analysis of the intracellular cycle. *J. Protozool.* 32, 80–83.
- Glaser, J., Schurigt, U., Suzuki, B.M., Caffrey, C.R., Holzgrabe, U., 2015. Anti-schistosomal activity of cinnamic acid esters: eugenyl and thymyl cinnamate induce cytoplasmic vacuoles and death in schistomula of *Schistosoma mansoni*. *Molecules* 20, 10873–10883.
- Gönnert, R., Andrews, P., 1977. Praziquantel, a new broad-spectrum antischistosomal agent. *Z. Parasitenkd.* 52, 129–150.
- Hotez, P.J., 2018. Human parasitology and parasitic diseases: heading towards 2050. *Adv. Parasitol.* 100, 29–38.
- Hotez, P.J., Brindley, P.J., Bethony, J.M., King, C.H., Pearce, E.J., Jacobson, J., 2008. Helminth infections: the great neglected tropical diseases. *J. Clin. Invest.* 118, 1311–1321.
- http://unitingtocombatntds.org/wp-content/themes/tetloose/app/staticPages/fifthReport/files/fifth_progress_report_english.pdf, 2014.
- Imai, K., Hayashi, Y., Hashimoto, K., 1981. Acute toxicological studies of captopril in rats and mice. *J. Toxicol. Sci.* 6 (Suppl. 2), 179–188.
- Jacobsen, W., Christians, U., Benet, L.Z., 2000. In vitro evaluation of the disposition of a novel cysteine protease inhibitor. *Drug Metab. Dispos.* 28, 1343–1351.
- Jaffe, I.A., 1986. Adverse effects profile of sulphydryl compounds in man. *Am. J. Med.* 80, 471–476.
- Kalgutkar, A.S., Gardner, I., Obach, R.S., Shaffer, C.L., Callegari, E., Henne, K.R., Mutlib, A.E., Dalvie, D.K., Lee, J.S., Nakai, Y., O'Donnell, J.P., Boer, J., Harriman, S.P., 2005. A comprehensive listing of bioactivation pathways of organic functional groups. *Curr. Drug Metabol.* 6, 161–225.
- Keiser, J., Chollet, J., Xiao, S.H., Mei, J.Y., Jiao, P.Y., Utzinger, J., Tanner, M., 2009. Mefloquine-an aminoalcohol with promising antischistosomal properties in mice. *PLoS Neglected Trop. Dis.* 3, e350.
- Kim, W., Kim, B.G., Lee, J.S., Lee, C.K., Yeon, J.E., Chang, M.S., Kim, J.H., Kim, H., Yi, S., Lee, J., Cho, J.Y., Kim, S.G., Lee, J.H., Kim, Y.J., 2017. Randomised clinical trial: the efficacy and safety of oltipraz, a liver X receptor alpha-inhibitory dithiolethione in patients with non-alcoholic fatty liver disease. *Aliment Pharmacol. Ther.* 45, 1073–1083.
- King, C.H., 2010. Parasites and poverty: the case of schistosomiasis. *Acta Trop.* 113, 95–104.
- Klayman, D.L., Gilmore, W.F., 1964. The synthesis of N-substituted 2-aminoethanethiosulfuric acids. *J. Med. Chem.* 7, 823–824.
- Klayman, D.L., Grenan, M.M., Jacobus, D.P., 1969a. Potential antiradiation agents. I. Primary aminoalkanethiosulfuric acids. *J. Med. Chem.* 12, 510–512.
- Klayman, D.L., Grenan, M.M., Jacobus, D.P., 1969b. Potential antiradiation agents. II. Guanidinoalkanethiosulfuric acids. *J. Med. Chem.* 12, 723–725.
- Kraemer, M., Vassy, J., Brighton, V., Fuller, S., Yeoh, G., 1986. The effect of dexamethasone on transferrin secretion by cultured fetal rat hepatocytes. *Eur. J. Cell Biol.* 42, 52–59.
- Lau, Y.Y., Sapidou, E., Cui, X., White, R.E., Cheng, K.C., 2002. Development of a novel in vitro model to predict hepatic clearance using fresh, cryopreserved, and sandwich-cultured hepatocytes. *Drug Metab. Dispos.* 30, 1446–1454.
- Lipinski, C.A., Lombardo, F., Dominy, B.W., Feeney, P.J., 2001. Experimental and computational approaches to estimate solubility and permeability in drug discovery and development settings. *Adv. Drug Deliv. Rev.* 46, 3–26.
- Long, T., Neitz, R.J., Beasley, R., Kalyanaraman, C., Suzuki, B.M., Jacobson, M.P., Dissous, C., McKerrow, J.H., Drewry, D.H., Zuercher, W.J., Singh, R., Caffrey, C.R., 2016. Structure-bioactivity relationship for benzimidazole thiophene inhibitors of polo-like kinase 1 (PLK1), a potential drug target in *Schistosoma mansoni*. *PLoS Neglected Trop. Dis.* 10, e0004356.
- Long, T., Rojo-Arreola, L., Shi, D., El-Sakkary, N., Jarnagin, K., Rock, F., Meewan, M., Rascon Jr., A.A., Lin, L., Cunningham, K.A., Lemieux, G.A., Podust, L., Abagyan, R.,

- Ashrafi, K., McKerrow, J.H., Caffrey, C.R., 2017. Phenotypic, chemical and functional characterization of cyclic nucleotide phosphodiesterase 4 (PDE4) as a potential anthelmintic drug target. *PLoS Neglected Trop. Dis.* 11, e0005680.
- Marcellino, C., Gut, J., Lim, K.C., Singh, R., McKerrow, J., Sakanari, J., 2012. WormAssay: a novel computer application for whole-plate motion-based screening of macroscopic parasites. *PLoS Neglected Trop. Dis.* 6 e1494.
- Mkoji, G.M., Smith, J.M., Prichard, R.K., 1990. Effect of oltipraz on the susceptibility of adult *Schistosoma mansoni* to killing by mouse peritoneal exudate cells. *Parasitol. Res.* 76, 435–439.
- Monks, T.J., Jones, D.C., 2002. The metabolism and toxicity of quinones, quinonimines, quinone methides, and quinone-thioethers. *Curr. Drug Metabol.* 3, 425–438.
- Moreira, L.S., Pilo-Veloso, D., de Mello, R.T., Coelho, P.M., Nelson, D.L., 2007. A study of the activity of 2-(alkylamino)-1-phenyl-1-ethanethiosulfuric acids against infection by *Schistosoma mansoni* in a murine model. *Trans. R. Soc. Trop. Med. Hyg.* 101, 385–390.
- Moreira, L.S., Piló-Veloso, D., Nelson, D.L., 2000. Synthesis of 2-(alkylamino)-1-phenylethane-1-thiosulfuric acids. potential schistosomicides *Quimica Nova* 23, 447–452.
- Nakabayashi, H., Taketa, K., Yamane, T., Miyazaki, M., Miyano, K., Sato, J., 1984. Phenotypic stability of a human hepatoma cell line, HuH-7, in long-term culture with chemically defined medium. *Gann* 75, 151–158.
- Nelson, D.L., Pellegrino, J., 1976. Experimental chemotherapy of schistosomiasis XII. Active derivatives of aminoethanethiosulfuric acids. *Rev. Inst. Med. Trop. Sao Paulo* 18, 365–370.
- Nelson, D.L., Veloso, D.P., Penido, M.L.O., Cardoso, M.G., Alcântara, A.F.C., 1989. Synthesis of potential schistosomicides: 2-(N-alkylamino)-1-alkanethiosulfuric acids and related thiols and disulfides. In: 31st National Organic Symposium, Ithaca, N Y, pp. 25.
- Nwaka, S., Hudson, A., 2006. Innovative lead discovery strategies for tropical diseases. *Nat. Rev. Drug Discov.* 5, 941–955.
- Pellegrino, J., Siqueira, A.F., 1956. A perfusion technic for recovery of *Schistosoma mansoni* from experimentally infected Guinea pigs. *Rev. Bras. Malariol. Doencas Trop.* 8, 589–597.
- Penido, M.L., Coelho, P.M., Nelson, D.L., 1999. Efficacy of a new schistosomicidal agent 2-[(methylpropyl)amino]-1-octanethiosulfuric acid against an oxamniquine resistant *Schistosoma mansoni* isolate. *Mem. Inst. Oswaldo Cruz* 94, 811–813.
- Penido, M.L., Nelson, D.L., Vieira, L.Q., Coelho, P.M., 1994. Schistosomicidal activity of alkylaminooctanethiosulfuric acids. *Mem. Inst. Oswaldo Cruz* 89, 595–602.
- Penido, M.L., Nelson, D.L., Vieira, L.Q., Watson, D.G., Kusel, J.R., 1995. Metabolism by *Schistosoma mansoni* of a new schistosomicide: 2-[(1-methylpropyl)amino]-1-octanethiosulphuric acid. *Parasitology* 111 (Pt 2), 177–185.
- Pica-Mattoccia, L., Cioli, D., 2004. Sex- and stage-related sensitivity of *Schistosoma mansoni* to in vivo and in vitro praziquantel treatment. *Int. J. Parasitol.* 34, 527–533.
- Rheinberg, C.E., Mone, H., Caffrey, C.R., Imbert-Establet, D., Jourdan, J., Ruppel, A., 1998. *Schistosoma haematobium*, *S. intercalatum*, *S. japonicum*, *S. mansoni*, and *S. rodhaini* in mice: relationship between patterns of lung migration by schistosomula and perfusion recovery of adult worms. *Parasitol. Res.* 84, 338–342.
- Rojo-Arreola, L., Long, T., Asarnow, D., Suzuki, B.M., Singh, R., Caffrey, C.R., 2014. Chemical and genetic validation of the statin drug target to treat the helminth disease, schistosomiasis. *PLoS One* 9, e87594.
- Rowland, A., Miners, J.O., Mackenzie, P.I., 2013. The UDP-glucuronosyltransferases: their role in drug metabolism and detoxification. *Int. J. Biochem. Cell Biol.* 45, 1121–1132.
- Sabah, A.A., Fletcher, C., Webbe, G., Doenhoff, M.J., 1986. *Schistosoma mansoni*: chemotherapy of infections of different ages. *Exp. Parasitol.* 61, 294–303.
- Sassine, A., Martins-Junior, H.A., Lebre, D.T., Valli, F., Pires, M.A., Vega, O., Felinto, M.C., 2008. An electrospray ionization tandem mass spectrometric study of p-tert-butylcalix[6]arene complexation with ammonium hydroxide, and ammonium and sodium ions. *Rapid Commun. Mass Spectrom.* 22, 385–393.
- Smith, R., Jones, R.D., Ballard, P.G., Griffiths, H.H., 2008. Determination of microsome and hepatocyte scaling factors for in vitro/in vivo extrapolation in the rat and dog. *Xenobiotica* 38, 1386–1398 the fate of foreign compounds in biological systems.
- Sohlenius-Sternbeck, A.K., 2006. Determination of the hepatocellularity number for human, dog, rabbit, rat and mouse livers from protein concentration measurements. *Toxicol. Vitro* 20, 1582–1586.
- Štefanić, S., Dvořák, J., Horn, M., Braschi, S., Sojka, D., Ruelas, D.S., Suzuki, B., Lim, K.C., Hopkins, S.D., McKerrow, J.H., Caffrey, C.R., 2010. RNA interference in *Schistosoma mansoni* schistosomula: selectivity, sensitivity and operation for larger-scale screening. *PLoS Neglected Trop. Dis.* 4 e850.
- Uttinger, J., N'Goran E, K., Caffrey, C.R., Keiser, J., 2011. From innovation to application: social-ecological context, diagnostics, drugs and integrated control of schistosomiasis. *Acta Trop.* 120 S121–137.
- Veber, D.F., Johnson, S.R., Cheng, H.Y., Smith, B.R., Ward, K.W., Kopple, K.D., 2002. Molecular properties that influence the oral bioavailability of drug candidates. *J. Med. Chem.* 45, 2615–2623.
- Venturello, C., Alneri, E., Ricci, M., 1983. A new, effective catalytic system for epoxidation of olefins by hydrogen peroxide under phase-transfer conditions. *J. Org. Chem.* 48, 3831–3833.
- Wang, P., Song, Y., Zhang, L., He, H., Zhou, X., 2005. Quinone methide derivatives: important intermediates to DNA alkylating and DNA cross-linking actions. *Curr. Med. Chem.* 12, 2893–2913.
- Weeks, J.C., Roberts, W.M., Leasure, C., Suzuki, B.M., Robinson, K.J., Currey, H., Wangchuk, P., Eichenberger, R.M., Saxton, A.D., Bird, T.D., Kraemer, B.C., Loukas, A., Hawdon, J.M., Caffrey, C.R., Liachko, N.F., 2018. Sertraline, paroxetine, and chlorpromazine are rapidly acting anthelmintic drugs capable of clinical repurposing. *Sci. Rep.* 8, 975.
- Williams, D.L., Bonilla, M., Gladyshev, V.N., Salinas, G., 2013. Thioredoxin glutathione reductase-dependent redox networks in platyhelminth parasites. *Antioxidants Redox Signal.* 19, 735–745.
- Xiao, S.H., Yue, W.J., Yang, Y.Q., You, J.Q., 1987. Susceptibility of *Schistosoma japonicum* to different developmental stages to praziquantel. *Chin Med J (Engl)* 100, 759–768.
- Zanger, U.M., Schwab, M., 2013. Cytochrome P450 enzymes in drug metabolism: regulation of gene expression, enzyme activities, and impact of genetic variation. *Pharmacol. Ther.* 138, 103–141.